AD-A131 710   A HIGH POWER OCTAVE BANDWIDTH I/J BAND CIRCULATOR(U)   1/1
RAYTHEON CO NORTHBOROUGH MA SPECIAL MICROWAVE DEVICES
OPERATION 31 DEC 81 N00173-80-C-0434

UNCLASSIFIED   F/G 9/1   NL

END
DATE
FILMED
9-83
DTIC

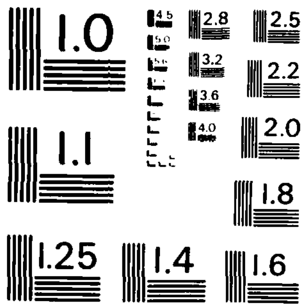

MICROCOPY RESOLUTION TEST CHART
NATIONAL BUREAU OF STANDARDS - 1963 - A

(2)

TECHNICAL REPORT

FINAL REPORT

FOR

A HIGH POWER OCTAVE BANDWIDTH

I/J BAND CIRCULATOR

Contract Number N00173-80-C-0434

For Period September 2, 1980 to December 31, 1981

Prepared For

Naval Research Laboratory
Washington, D.C. 20375

Prepared By

Raytheon Company
Special Microwave Devices Operation
5 Bearfoot Road
Northborough, MA 01532

SPECIAL MICROWAVE DEVICES OPERATION

RAYTHEON MICROWAVE AND POWER TUBE DIVISION

FINAL REPORT

FOR

A HIGH POWER OCTAVE BANDWIDTH

I/J BAND CIRCULATOR

Contract Number N00173-80-C-0434

For Period September 2, 1980 to December 31, 1981

Prepared For

Naval Research Laboratory
Washington, D.C. 20375

Prepared By

Raytheon Company
Special Microwave Devices Operation
5 Bearfoot Road
Northborough, MA 01532

TABLE OF CONTENTS

LIST OF ILLUSTRATIONS

LIST OF ILLUSTRATIONS (CONT'D)

1.0 INTRODUCTION

This report describes the results achieved for the development of a circulator under Contract N00173-80-C-0434. This program called for the development of an octave band circulator in 7.5 - 18 GHz having the following specifications.

	Design Objectives	Proposed
Frequency Range	7.5 - 18	7.5 - 18
Instantaneous Bandwidth	1 Octave	1 Octave
Power Levels		
Peak Power	20 kW Min.	20 kW Min.
Average Power	1 kW Min.	1 kW Min.
Isolation	20 dB Min.	20 dB Min. (70% of band) 18 dB Min.
Insertion Loss	0.6 dB Max.	0.6 dB (70% of band) 0.7 dB Max.
VSWR		
VSWR Into Matched Load	1.15	1.25 (70% of band) 1.35 Max.
Max Load VSWR	2.0:1	2.0:1
Temperature Range	0 to 50°C	0 to 50°C
Waveguide Inputs	WRD750D24	WRD750D24
Number of Accessible Ports	4	4
Applied Field	Fixed Magnets	Fixed Magnets
Cooling	-	Liquid
Flow	-	1/4 gpm
Pressure Drop	-	10 psi

Initially, a four port differential phase shift circulator using nonreciprocal phase shifter in a rectangular waveguide structure was studied. Nonreciprocal phase shifter design with H-plane ferrite and E-plane dielectric in a rectangular waveguide displayed limitations in terms of broadband performance. With optimum phase shifter geometry, 90% of required bandwidth could be achieved. However matching section of phase shifter and transition from rectangular to ridge waveguide would further limit the bandwidth. Therefore, the phase shifter design using rectangular waveguide was abandoned and nonreciprocal phase shifters in double ridge waveguide structures were used in the circulator design.

During the course of the circulator development program analytical studies on dielectric and ferrite loaded double ridge waveguide were performed. Design effort was placed on the frequency range between 8 to 16 GHz. Raytheon circulator design uses two magic tees and two non-identical nonreciprocal phase shifters in standard WRD750D24 double ridge waveguide.

2.0 CIRCULATOR CONFIGURATIONS

Differential phase shift circulators can be built in several configurations. Four configurations are shown in Figure 1 (a), (b), (c), and (d). All four have the same principle of operations. Power entering Port 1 emerges from Port 2 only, and so on until power entering Port 4 emerges from Port 1 only.

The device in Figure 1(a) is the most common configuration. This option is probably the most favorable if a 3 dB quadrature hybrid operating over the required frequency range with acceptable unbalance is available. Unfortunately a 3 dB quadrature hybrid at the desired frequency range with suitable performance is not currently available. The design indicated in Figure 1(b) uses input and output magic tees, separated by a $0^{\circ}/180^{\circ}$ nonreciprocal phase shifter in parallel with a dielectrically loaded reciprocal tracking phase shifter. The design of $0^{\circ}/180^{\circ}$ nonreciprocal phase shifters requires longer ferrite slab, hence, causing higher insertion loss of the phase shifter. The circulator design using Figure 1(b) causes an amplitude unbalance because the insertion loss of the ferrite is higher than that of the dielectric. The design in Figure 1(c) uses two magic tees, two identical $0^{\circ}/90^{\circ}$ nonreciprocal phase shifters, and two dielectrically loaded reciprocal phase shifters which provide a fixed reciprocal phase difference of 90° between the two phase shifters over the operating frequency range. For wideband design, the reciprocal phase shifters imposes serious limitations on the

bandwidth because a phase shift of approximately 90° cannot be maintained across a wide range of frequencies. The approach using Figure 1(d) uses two magic tees and two non-identical nonreciprocal phase shifters. Phase tracking requirement over wide bandwidth can be met more easily using this technique. This approach was used in our design. Scattering matrix analysis for this configuration is shown in the next section.

2.1 Scattering Matrix Analysis of Circulator

Dynamic behavior of a four port differential phase shift circulator can be described using scattering matrix analysis. Employing scattering matrix, wave amplitude emerging from all four ports can be described as a function of input wave amplitude and scattering parameters of all the interconnected devices. Figure 2 shows four port differential phase shift circulator configuration used for anlaysis. Instead of using a conventional S-parameter notation such as S_{ij}, a slightly different notation is used in this analysis. They are defined as follows:

X_i - indicates wave amplitude entering into Port i of the magic tee 1.

x_i - indicates wave amplitude leaving from port i of the magic tee 1.

a_{ij} - indicates scattering parameter of the magic tee 1.

Y_i - indicates wave amplitude entering into Port i of the magic tee 2.

y_i - indicates wave amplitude leaving from Port i of the magic tee 2.

b_{ij} - indicates scattering parameter of the magic tee 2.

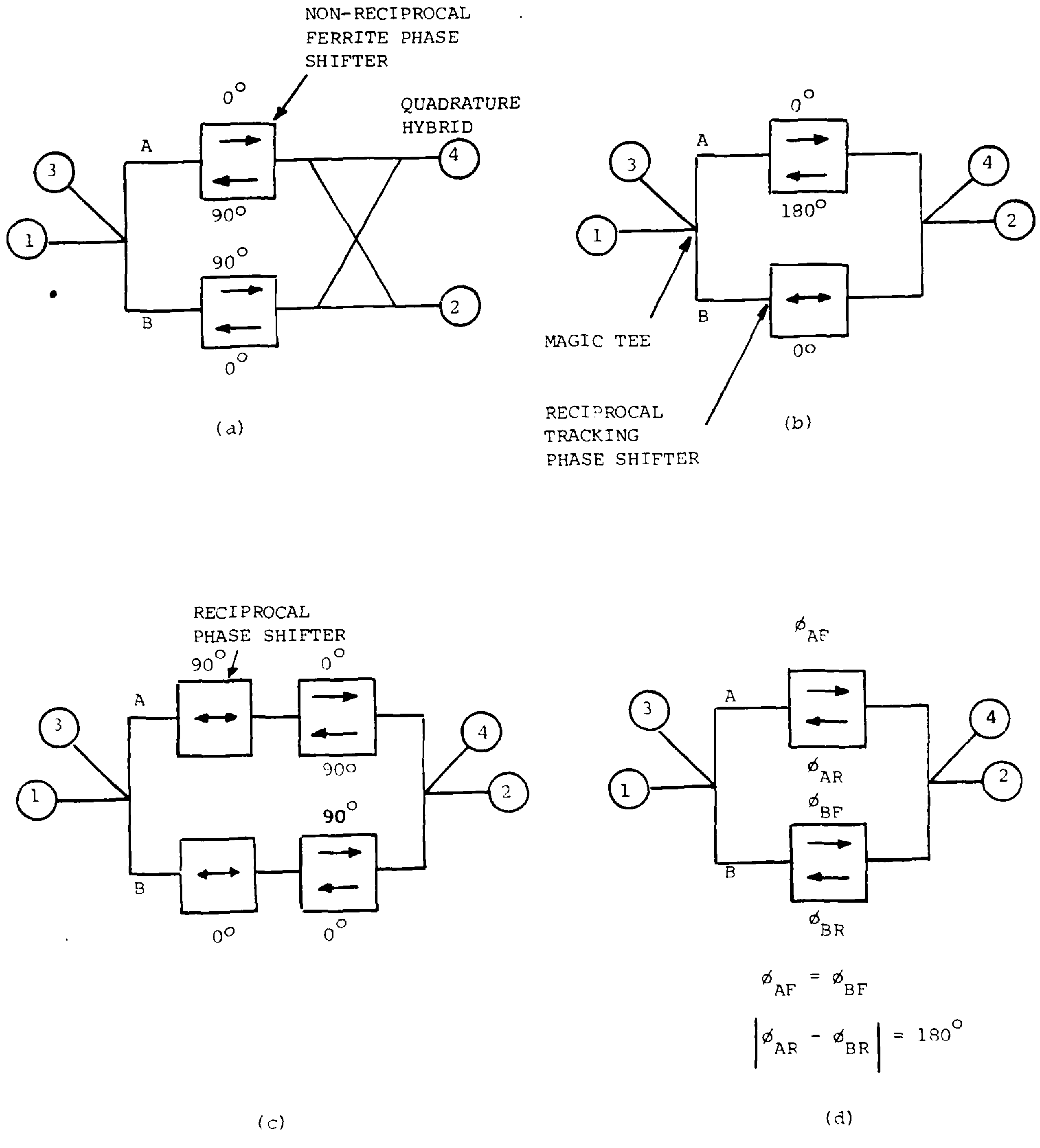

Figure 1. Circulator Configurations

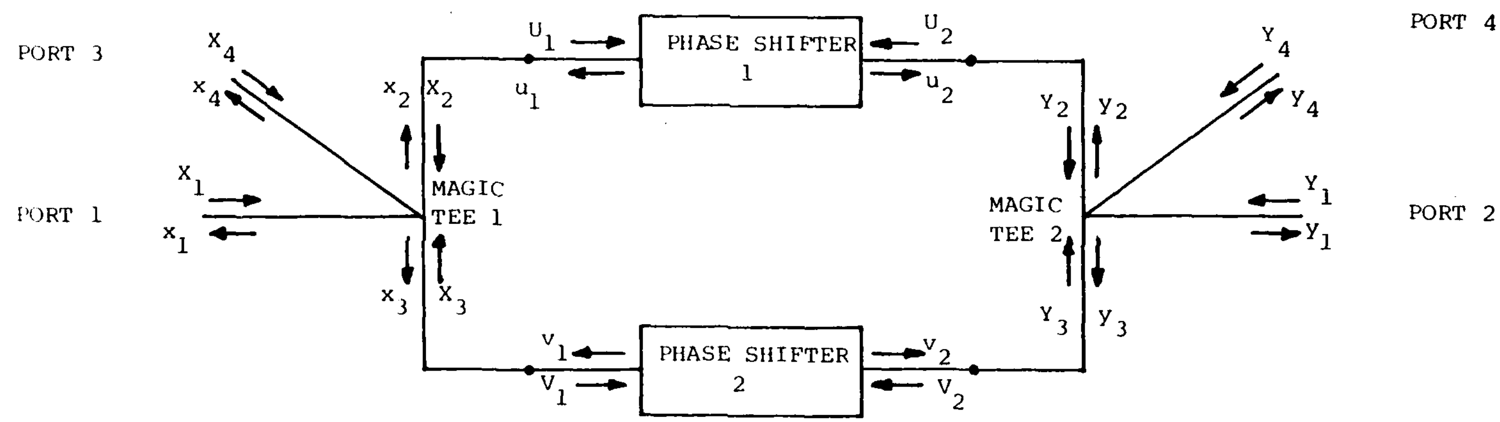

Figure 2. Circulator Configuration for Scattering Matrix Analysis

U_i - indicates wave amplitude entering into Port i of the phase shifter 1.

u_i - indicates wave amplitude leaving from Port i of the phase shifter 1.

c_{ij} - indicates scattering parameter of the phase shifter 1.

V_i - indicates wave amplitude entering into Port i of the phase shifter 2.

v_i - indicates wave amplitude leaving from port i of the phase shifter 2.

d_{ij} - indicates scattering parameter of the phase shifter 2.

All of the parameters defined above are complex quantities involving magnitude and phase. According to the notations given above, each device can be expressed as:

$$\begin{bmatrix} x_1 \\ x_2 \\ x_3 \\ x_4 \end{bmatrix} = \begin{bmatrix} a_{11} & a_{12} & a_{13} & a_{14} \\ a_{21} & a_{22} & a_{23} & a_{24} \\ a_{31} & a_{32} & a_{33} & a_{34} \\ a_{41} & a_{42} & a_{43} & a_{44} \end{bmatrix} \begin{bmatrix} X_1 \\ X_2 \\ X_3 \\ X_4 \end{bmatrix} \quad \text{For magic tee 1} \qquad (1)$$

$$\begin{bmatrix} y_1 \\ y_2 \\ y_3 \\ y_4 \end{bmatrix} = \begin{bmatrix} b_{11} & b_{12} & b_{13} & b_{14} \\ b_{21} & b_{22} & b_{23} & b_{24} \\ b_{31} & b_{32} & b_{33} & b_{34} \\ b_{41} & b_{42} & b_{43} & b_{44} \end{bmatrix} \begin{bmatrix} Y_1 \\ Y_2 \\ Y_3 \\ Y_4 \end{bmatrix} \quad \text{For magic tee 2} \qquad (2)$$

$$\begin{bmatrix} u_1 \\ u_2 \end{bmatrix} = \begin{bmatrix} c_{11} & c_{12} \\ c_{21} & c_{22} \end{bmatrix} \begin{bmatrix} U_1 \\ U_2 \end{bmatrix} \quad \text{For phase shifter 1} \qquad (3)$$

$$\begin{bmatrix} v_1 \\ v_2 \end{bmatrix} = \begin{bmatrix} d_{11} & d_{12} \\ d_{21} & d_{22} \end{bmatrix} \begin{bmatrix} V_1 \\ V_2 \end{bmatrix} \quad \text{For phase shifter 2} \qquad (4)$$

And we have the following relations:

$$
\begin{aligned}
X_2 &= u_1 \\
X_3 &= v_1 \\
Y_2 &= u_2 \\
Y_3 &= v_2
\end{aligned}
\tag{5}
$$

$$
\begin{aligned}
U_1 &= x_2 \\
U_2 &= y_2 \\
V_1 &= x_3 \\
V_2 &= y_3
\end{aligned}
\tag{6}
$$

We can identify X_1, X_4, Y_1, and Y_4 as input wave amplitude of the circulator and x_1, x_4, y_1, and y_4 as output wave amplitude of the circulator.

Using equations (1) through (6), any output wave amplitude can be expressed as a function of input wave amplitude and scattering parameters of all the interconnected devices.

For example, if we consider Port 1 as an input port then:

$$X_4 = Y_1 = Y_4 = 0 \tag{7}$$

and output wave amplitude can be written as:

$$
\begin{aligned}
x_1 &= a_{11}X_1 + a_{12}\,(c_{11}x_2 + c_{12}y_2) + a_{13}\,(d_{11}x_3 + d_{12}y_3) \\
x_4 &= a_{41}X_1 + a_{42}\,(c_{11}x_2 + c_{12}y_2) + a_{43}\,(d_{11}x_3 + d_{12}y_3) \\
y_1 &= b_{12}\,(c_{21}x_2 + c_{22}y_2) + b_{13}\,(d_{21}x_3 + d_{22}y_3) \\
y_4 &= b_{42}\,(c_{21}x_2 + c_{22}y_2) + b_{43}\,(d_{21}x_3 + d_{22}y_3)
\end{aligned}
\tag{8}
$$

where x_2, x_3, y_2, and y_3 can be obtained by solving the following simultaneous equations:

$$\begin{bmatrix} (1-a_{22}c_{11}) & -a_{23}d_{11} & -a_{22}c_{12} & -a_{23}d_{12} \\ -a_{32}c_{11} & (1-a_{33}d_{11}) & -a_{32}c_{12} & -a_{33}d_{12} \\ -b_{22}c_{21} & -b_{23}d_{21} & (1-b_{22}c_{22}) & -b_{23}d_{22} \\ -b_{32}c_{21} & -b_{33}d_{21} & -b_{32}c_{22} & (1-b_{33}d_{22}) \end{bmatrix} \begin{bmatrix} x_2 \\ x_3 \\ y_2 \\ y_3 \end{bmatrix} = \begin{bmatrix} a_{21}X_1 \\ a_{31}X_1 \\ 0 \\ 0 \end{bmatrix} \tag{9}$$

Similarly, we can obtain all the output wave amplitude involving with different input port.

If we assume ideal magic tee, scattering matrix of ideal magic tee can be written as:

$$\begin{bmatrix} 0 & 1/\sqrt{2} & 1/\sqrt{2} & 0 \\ 1/\sqrt{2} & 0 & 0 & 1/\sqrt{2} \\ 1/\sqrt{2} & 0 & 0 & -1/\sqrt{2} \\ 0 & 1/\sqrt{2} & -1/\sqrt{2} & 0 \end{bmatrix} \tag{10}$$

and the equation (8) can be reduced to:

$$
\begin{aligned}
x_1 &= \frac{X_1}{2}(c_{11} + d_{11}) \\
x_4 &= \frac{X_1}{2}(c_{11} - d_{11}) \\
y_1 &= \frac{X_1}{2}(c_{21} + d_{21}) \\
y_4 &= \frac{X_1}{2}(c_{21} - d_{21})
\end{aligned}
\qquad (11)
$$

3.0 FERRITE MATERIAL

Choice of a ferrite material for our application involves the following considerations.

(a) The material should be reproducible on a piece to piece basis - particularly free from density variations and $4\pi M_s$ variations.

(b) The material should, when used in the device, have acceptably low rf magnetic loss at both low signal strength and high signal strength (i.e., not exhibit nonlinear loss mechanisms).

(c) The material should have a low temperature coefficient of magnetization - this normally implies a Curie temperature in excess of $300^\circ C$.

(d) The ratio $\gamma 4\pi M_s/W$ should be between 0.4 and 0.8. Below 0.4 the phase shift per unit length becomes too low, above 0.8 the ferrite exhibits low field loss.

Of the basic families of ferrite materials that are available (hybrid garnets, magnesium manganese, spinels, lithium ferrites and nickel ferrites) nickel ferrites are most useful at the frequency range and power level in consideration. They have high Curie temperature (greater than $450^\circ C$), suitable magnetization (1500 Gauss to 3100 Gauss) and acceptable magnetic loss. C-20 nickel ferrite material from Countis Industries was used for circulator design.

4.0 *PHASE SHIFTER*

4.1 Theoretical Analysis

Theoretical analysis was performed on dielectric and ferrite loaded ridge waveguide. The geometry under study is shown in Figure 3. Dielectric rib is fully extending across the ridge gap, and ferrite slabs are partially extending across the ridge gap. Exact solution to the given problem is very difficult to obtain, if not impossible. To approximate propagation constant of the dominant mode, transverse resonace equation was derived employing ABCD matrix method.[1]

In ABCD matrix method, the electric field in the z direction and magnetic field in the y direction at x = 0 are related to the electric field in the z direction and the magnetic field in the y direction at x = a by an ABCD matrix as

$$\begin{bmatrix} Hy\ (x = a) \\ Ez\ (x = a) \end{bmatrix} = \begin{bmatrix} A & B \\ C & D \end{bmatrix} \begin{bmatrix} Hy\ (x = 0) \\ Ez\ (x = 0) \end{bmatrix} \qquad (1)$$

Because the electric fields at the waveguide walls are zero, equation (1) can be written as:

$$\begin{bmatrix} Hy\ (x = a) \\ 0 \end{bmatrix} = \begin{bmatrix} A & B \\ C & D \end{bmatrix} \begin{bmatrix} Hy\ (x = 0) \\ 0 \end{bmatrix}$$

[1] "TE-Mode Solutions for Partially Ferrite Filled Rectangular Waveguide Using ABCD Matrices", W.P. Clark, K.H. Hering, D.A. Charlton, MTT 1966.

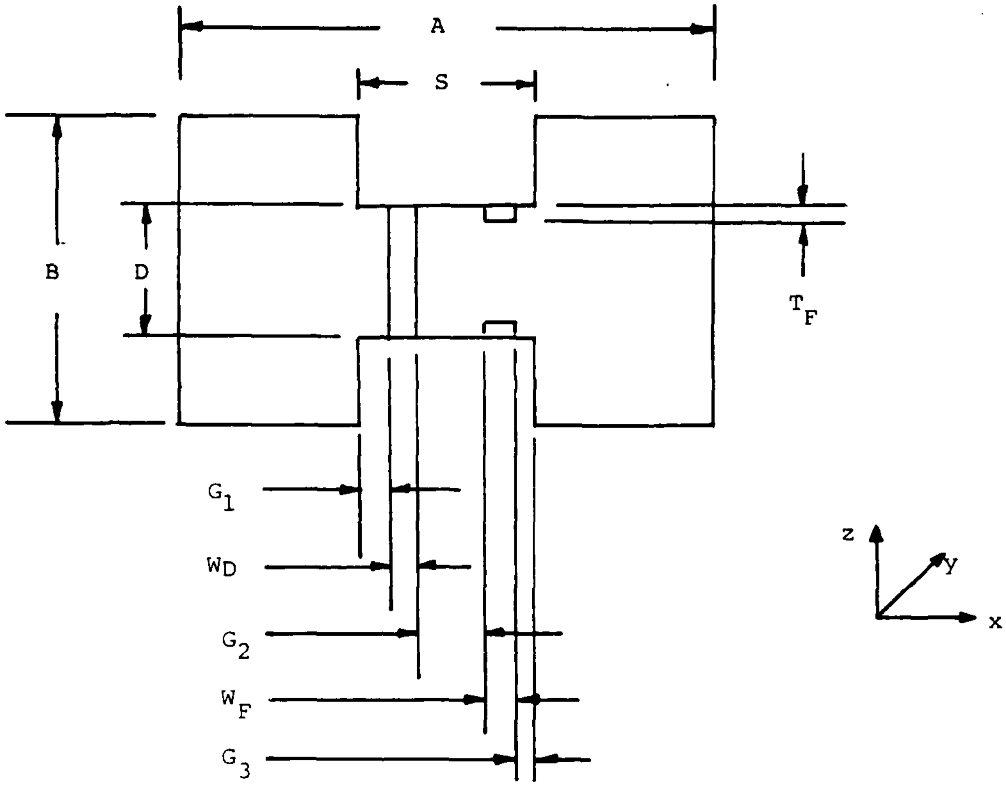

Figure 3. Dielectric and Ferrite Loaded Double Ridge Waveguide

or,

$$Hy\ (x = a) = A\ Hy\ (x = 0) \tag{2a}$$

$$0 = C\ Hy\ (x = 0) \tag{2b}$$

For nontrivial solution, the matrix term C must be zero. Therefore, the transverse resonance equation requires

$$C = 0 \tag{3}$$

By applying the ABCD method to each region in Figure 3, the matrix quantity C can be calculated as follows:

$$\begin{bmatrix} A & B \\ C & D \end{bmatrix} = \begin{bmatrix} A_1 & B_1 \\ C_1 & D_1 \end{bmatrix} \begin{bmatrix} A_2 & B_2 \\ C_2 & D_2 \end{bmatrix} \cdots \begin{bmatrix} A_n & B_n \\ C_n & D_n \end{bmatrix} \tag{4}$$

ABCD matrix for each region can be represented as

i) Dielectric Region (including air)

$$A = \cos K_x \ell \tag{5a}$$

$$B = -j \frac{K_x}{\omega \mu_o} \sin K_x \ell \tag{5b}$$

$$C = -j \frac{\omega \mu_o}{K_x} \sin K_x \ell \tag{5c}$$

$$D = \cos K_x \ell \tag{5d}$$

where $K_x^2 = K_o^2 \varepsilon - \beta^2$ (6)

ℓ is the width of the region

ii) Ferrite region (Ho and Mo are in +z direction)

$$A = \cos K_{xf}\ell - \frac{j\beta}{K_{xf}\theta} \operatorname{Sin} K_{xf}\ell \tag{7a}$$

$$B = \frac{j\rho}{\omega\mu K_{xf}} \left(\frac{\beta^2}{\theta^2} - K_{xf}^2\right) \operatorname{Sin} K_{xf}\ell \tag{7b}$$

$$C = \frac{-j\,\omega\mu}{\rho K_{xf}} \operatorname{Sin} K_{xf}\ell \tag{7c}$$

$$D = \cos K_{xf}\ell + \frac{j\beta}{K_{xf}\theta} \operatorname{Sin} K_{xf}\ell \tag{7d}$$

where $$K_{xf}^2 = \frac{\omega^2\mu\varepsilon_f}{\rho} - \beta^2 \tag{8}$$

$$\rho = \frac{1+\chi_{xx}}{(1+\chi_{xx})^2 + \chi_{xy}^2} \tag{9a}$$

$$\theta = \frac{1+\chi_{xx}}{\chi_{xy}} \tag{9b}$$

$$\chi_{xx} = \frac{(\gamma 4\pi Mo)\ (\gamma Ho)}{(\gamma Ho)^2 - \omega^2} \tag{10a}$$

$$\chi_{xy} = \frac{-j(\gamma 4\pi Mo)\omega}{(\gamma Ho)^2 - \omega^2} \tag{10b}$$

γ is the electron gyromagnetic ratio

Mo is the ferrite magnetization

Ho is the internal DC magnetic field

ω is the angular frequency of the electromagnetic field.

If Ho and Mo are in -z direction, χ_{xx} is unchanged and χ_{xy} changes sign.

In the region where the internal DC magnetic field is small compared to the angular frequency, equation (10) can be simplified as

$$\chi_{xx} \simeq 0 \tag{11a}$$

$$\chi_{xy} \simeq j\,\frac{\gamma 4\pi M_o}{\omega} \tag{11b}$$

iii) <u>Height change (See Figure 4)</u>

When the height of the transmission line in the transverse plane changes from b to d, ABCD matrix can be written as

$$A = d/b \tag{12a}$$

$$B = 0 \tag{12b}$$

$$C = 0 \tag{12c}$$

$$D = 1 \tag{12d}$$

iv) <u>Junction Capacitance (See Figure 4)</u>

The ridge in the waveguide presents discontinuities to the electromagnetic waves and causes local fields. The effects of these local fields are capacitive in nature and included in the transmission line as discontinuity susceptance. ABCD matrix can be written as

$$A = 1 \tag{13a}$$

$$B = B_c \tag{13b}$$

$$C = 0 \tag{13c}$$

$$D = 1 \tag{13d}$$

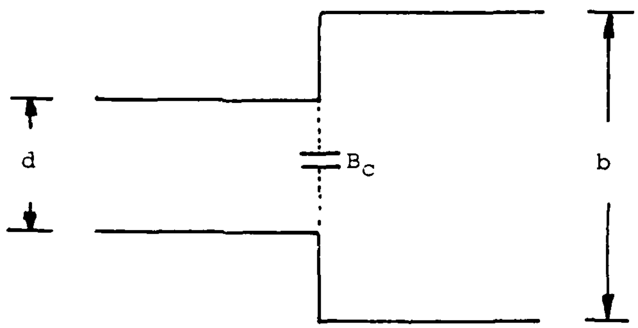

Figure 4. Transmission Line Model for Height Change and Junction Capacitance

Where jB_c is capacitive junction susceptance. The value of B_c can be obtained from the equation below.[2]

$$\frac{B_c}{Y_{ol}} = \frac{2b}{\lambda_g}\left[\ell n\left(\frac{1-\alpha^2}{4\alpha}\right)\left(\frac{1+\alpha}{1-\alpha}\right)^{(\alpha+1/\alpha)/2} + 2\,\frac{(A + A' + 2C)}{AA' - C^2} + \left(\frac{b}{4\lambda_g}\right)^2\left(\frac{1-\alpha}{1+\alpha}\right)^{4\alpha}\left(\frac{5\alpha^2-1}{1-\alpha^2} + \frac{4\alpha^2 C}{3A}\right)^2\right] \tag{14}$$

Where
$$A = \left(\frac{1+\alpha}{1-\alpha}\right)^{2\alpha}\frac{1+\sqrt{1-(b/\lambda_g)^2}}{1-\sqrt{1-(b/\lambda_g)^2}} - \frac{1+3\alpha^2}{1-\alpha^2} \tag{15a}$$

$$A' = \left(\frac{1+\alpha}{1-\alpha}\right)^{2/\alpha}\frac{1+\sqrt{1-(d/\lambda_g)^2}}{1-\sqrt{1-(d/\lambda_g)^2}} + \frac{3+\alpha^2}{1-\alpha^2} \tag{15b}$$

$$C = \left(\frac{4\alpha}{1-\alpha^2}\right)^2 \tag{15c}$$

$$\alpha = d/b \tag{15d}$$

$$\lambda_g = \frac{2\pi}{K_{x1}} \tag{15e}$$

$$Y_{ol} = -\frac{K_{x1}}{\omega\mu_o} \tag{15f}$$

$$K_{x1} = \sqrt{K_o^2\varepsilon_o - \beta^2} \tag{15g}$$

Note: The value of Bc obtained from equation (14) assumes homogeneous loading of dielectric in the ridge waveguide. In case of inhomogeneous loading of dielectric in the ridge waveguide, the value of Bc may be used as crude approximation.

[2] "Waveguide Handbook", N. Marcuvitz, McGraw-Hill, 1951.

The solution for the propagation constant of the geometry shown in Figure 3 was programmed for the Hewlett Packard 9845 desk top computer. A copy of that program is included as Appendix B of this report.

In the preceeding analysis it was assumed that the ferrite region was fully filled. In practice it will only be partially filled in a high power circulator. It was found that an averaging technique could be used to adequately represent the partially loaded ferrite structure. The approximate values were determined by a set of iterations comparing analysis with measured results.

4.2 Phase Tracking

To implement the design of a four port differential phase shift circulator using two magic tees and two non-identical nonreciprocal phase shifters as shown in Figure 1(d), the following conditions are imposed upon the phase shifters:

$$\phi_{AF} = \phi_{BF} \tag{16}$$

$$\phi_{AR} - \phi_{BR} = 180^{\circ} \tag{17}$$

where:

ϕ_{AF} is insertion phase of Phase Shifter A in forward direction.

ϕ_{BF} is insertion phase of Phase Shifter B in forward direction.

ϕ_{AR} is insertion phase of Phase Shifter A in reverse direction.

ϕ_{BR} is insertion phase of Phase Shifter B in reverse direction.

Due to the frequency dependence of phase characteristics, these requirements are difficult to meet over wideband.

There are many parameters which can effect insertion phase, such as width of the dielectric rib, dielectric constant, location of dielectric rib, dimension and location of ferrite slab, and biasing magnetic field strength. To meet the phase tracking requirement, the insertion phase differential of the two phase shifters at demagnetized state should be

reasonably uniform over frequency range, preferably about 90^{o}. The choice of the dielectric constant and the width of the dielectric rib have the most significant effect in setting the proper amount of insertion phase differential. Typical insertion phase characteristics of dielectric and ferrite loaded phase shifter in WRD750D24 double ridge waveguide are shown in Figures 5 and 6. Two phase states due to oppositely directed biasing magnetic field are shown along with demagnetized phase state. Here we define longer phase state as β^- state and shorter phase state as β^+ state. The insertion phase characteristics of an empty WRD750D24 double ridge waveguide is also shown in the figures. In Figure 5, two phase shifters having the same dielectric constant are compared with respect to the variations in the width of the dielectric rib. In Figure 6, two phase shifters having the same width of dielectric rib are compared with respect to the variations in dielectric constant.

The phase tracking requirement given in equations (16) and (17) can be satisfied if we design the two phase shifters in such a way that:

i) The insertion phase of one phase shifter, say phase shifter A, in β^+ state is equal to the insertion phase of another phase shifter, say phase shifter B, in β^- state over the operating frequency range.

ii) The insertion phase of phase shifter A in β^- state is 180^{o} degree longer than that of phase shifter B in β^+ state over the operating frequency range.

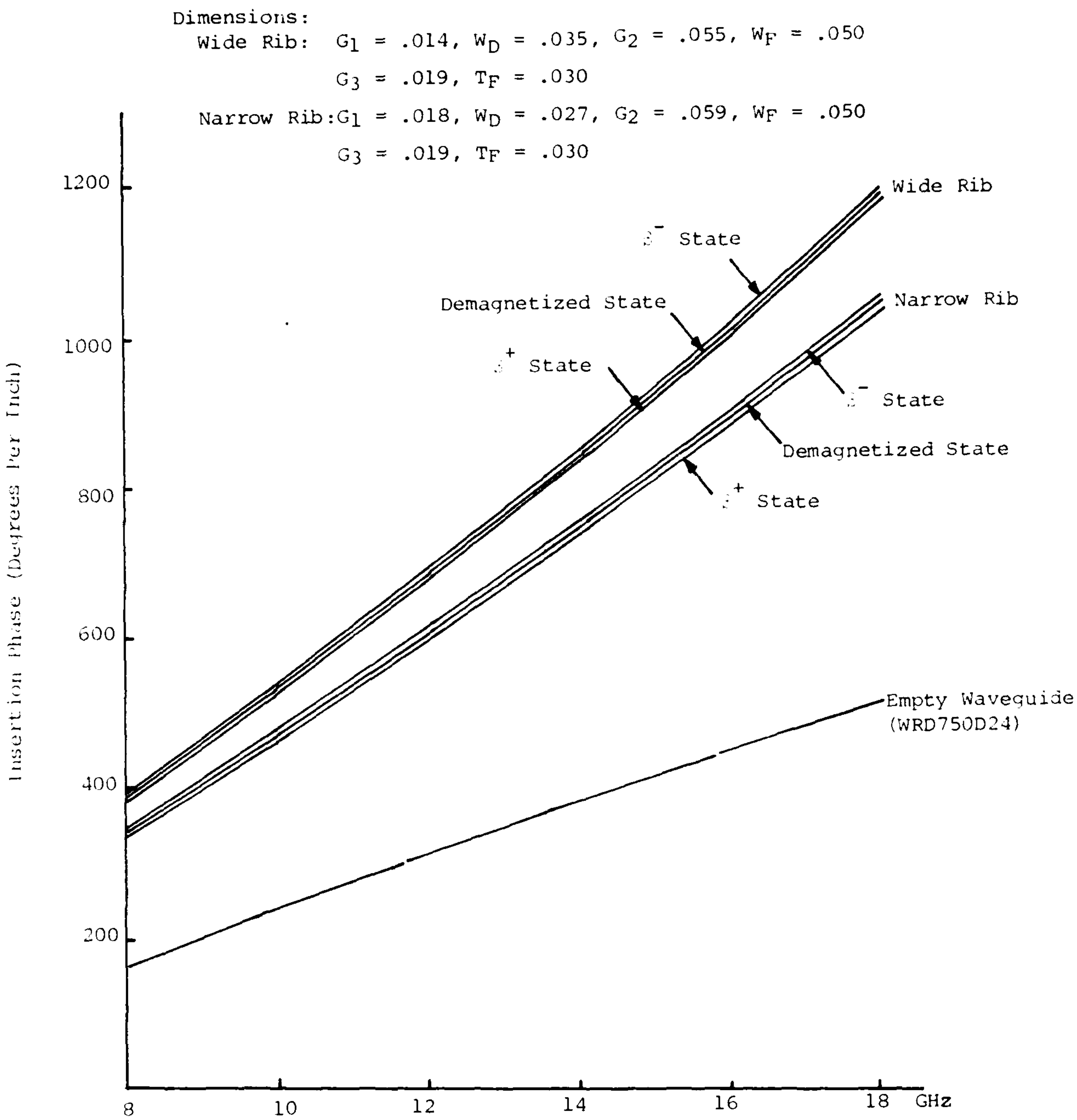

Figure 5. Phase Characteristics With Variations in the Width of Dielectric Rib (Dielectric Constant = 13)

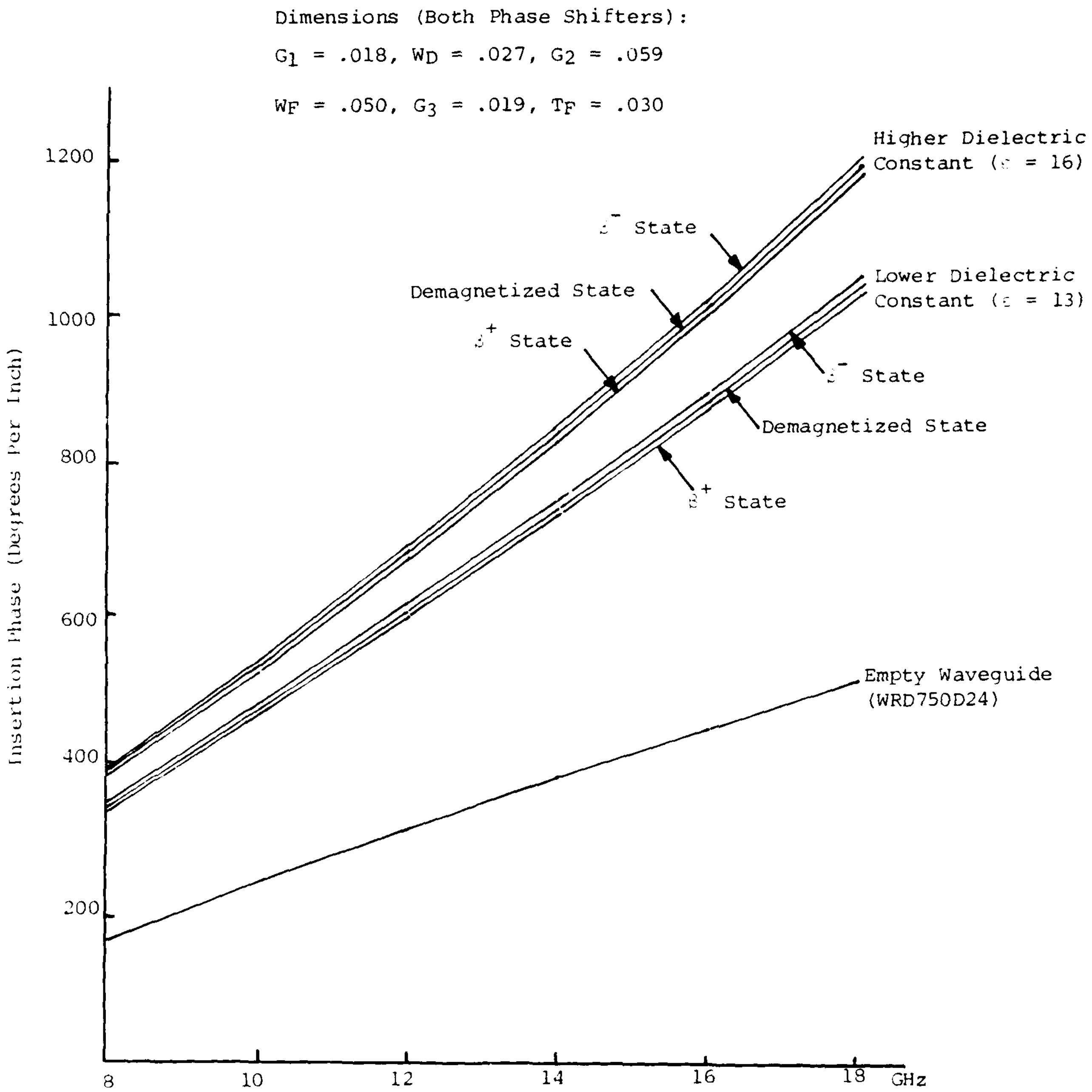

Figure 6. Phase Characteristics With Variations in the Dielectric Constant (Width of Dielectric Rib W_D = .027")

It can be accomplished by employing one phase shifter with shorter but wide dielectric rib (or higher dielectric constant) and another phase shifter with longer but narrow dielectric rib (or lower dielectric constant). The difference in length between these two sections is made up by length difference in the waveguide employed. The effect due to the insertion of matching transformers can be minimized by designing transformers having approximately the same insertion phase length for both phase shifters. Small insertion phase difference due to the matching transformer can be easily corrected by adjusting other parameter, such as location of dielectric rib and biasing magnetic field strength. Neglecting matching transformer, actual insertion phase differential of the two phase shifters at demagnetized state becomes:

$$\phi = \phi_N L_N - (\phi_W L_W + \phi_A L_A)$$

where ϕ_W is the phase length of wide phase shifter per inch at demagnetized state

ϕ_N is the phase length of narrow phase shifter per inch at demagnetized state

ϕ_A is the phase length of empty normal waveguide per inch

L_W is the physical length of wide phase shifter

L_N is the physical length of narrow phase shifter

L_A is the physical length of empty normal waveguide

$L_N = L_W + L_A$

By making adjustment of length, optimum result for uniform insertion phase differential can be obtained.

Once insertion phase differential is set within the acceptable range, fine adjustment can be made by adjusting location of dielectric rib and ferrite slab, and biasing H_{DC} field strength. Typical differential phase characteristics between δ^- state and δ^+ state with respect to the location of the dielectric rib is shown in Figure 7(a) and (b). When the dielectric rib is placed near the center of the ridge, it gives more differential phase at higher frequency. When the dielectric rib is moved toward the side, it gives more differential phase at lower frequency.

In practice, breadboard phase shifters were built based on computation, and absolute phase measurement was performed with variations in the width of dielectric rib, dielectric constant, location of dielectric and ferrite, and H_{DC} field strength. A simple computer program was written, and measured phase data were fed into the computer program to find optimum geometry. Introduction of matching sections introduced small deviation from optimum result, but compensation was done by adjusting the location of the dielectric rib.

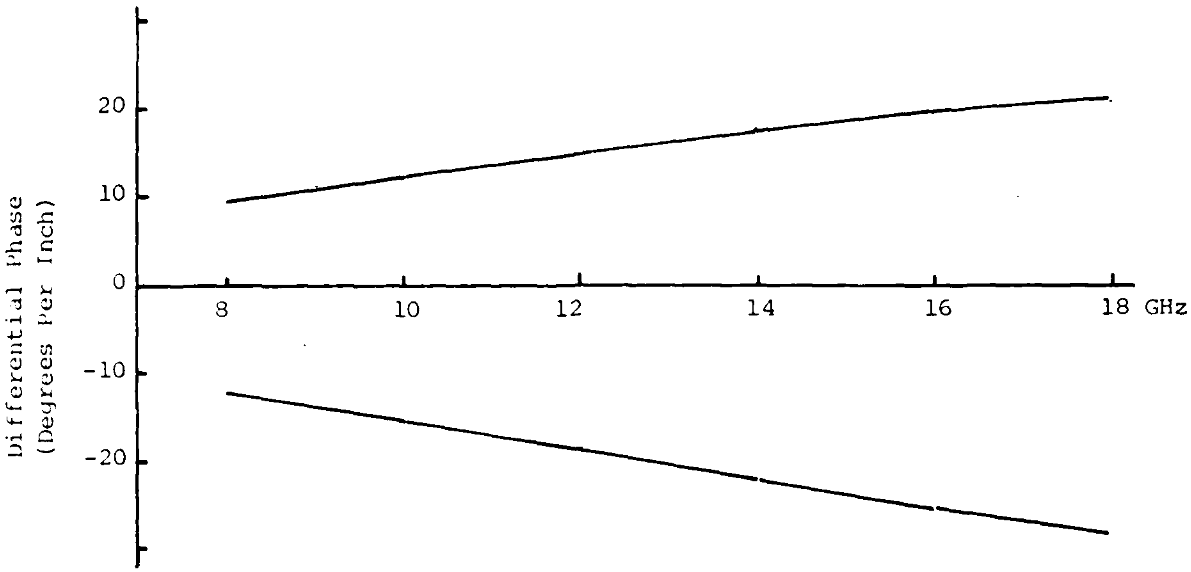

Figure 7(a). Differential Phase; Dielectric Rib is Loaded at the Center of the Ridge (WRD750D24)

G_1 = .069, W_D = .035, G_2 = 0, W_F = .050

G_3 = .019, T_F = .030, ϵ = 13

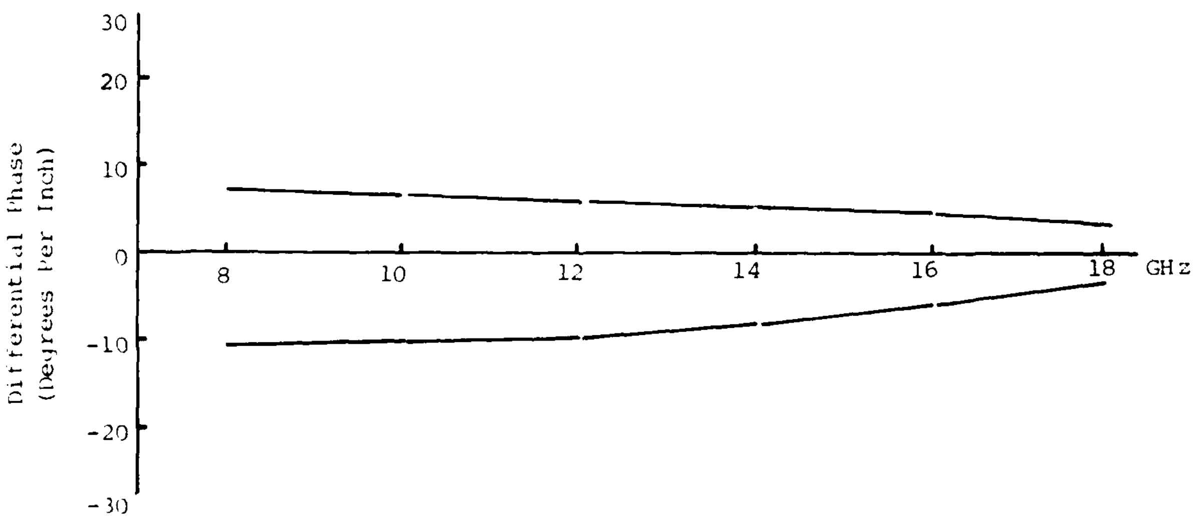

Figure 7(b). Differential Phase; Dielectric Rib is Loaded Near the Edge of the Ridge (WRD750D24)

G_1 = .014, W_D = .035, G_2 = .055, W_F = .050

G_3 = .019, T_F = .030, ϵ = 13

Figure 8 shows the actual dimension for phase shifters, and experimental results on phase are shown in Figure 9. (Note: Sign is inverted on phase scale, that is, bottom side has longer phase).

4.3 Matching

Chebyshev type 3 section dielectric loaded quarter wave transformers are utilized for both phase shifters. As mentioned above, the insertion of the matching transformers introduced small deviation from optimum result. By adjusting the location of the dielectric rib slightly, optimum result was obtained. Results on VSWR for both phase shifters are shown in Figures 10 and 11.

4.4 Insertion Loss

Figures 12 and 13 show total insertion loss for both phase shifters. These measurements include the line lengths of waveguide employed. Insertion loss can be reduced to some degree by improving VSWR and using low loss bonding material.

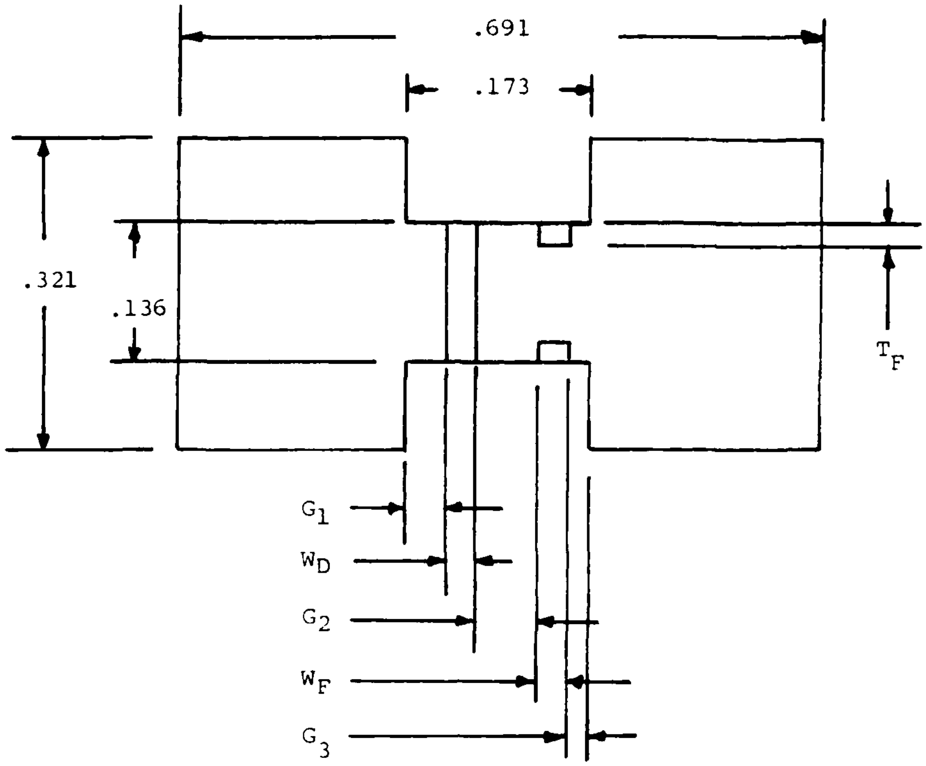

	PHASE SHIFTER A	PHASE SHIFTER B
G_1	.010"	.025"
W_D (Width of Dielectric Rib)	.035"	.0225"
G_2	.058"	.0455"
W_F (Width of Ferrite Slab)	.050"	.050"
G_3	.020"	.030"
T_F (Thickness of Ferrite Slab)	.030"	.030"
Length	3.890"	5.090"
Dielectric Constant	13	16

Figure 8. Dimensions for Phase Shifters

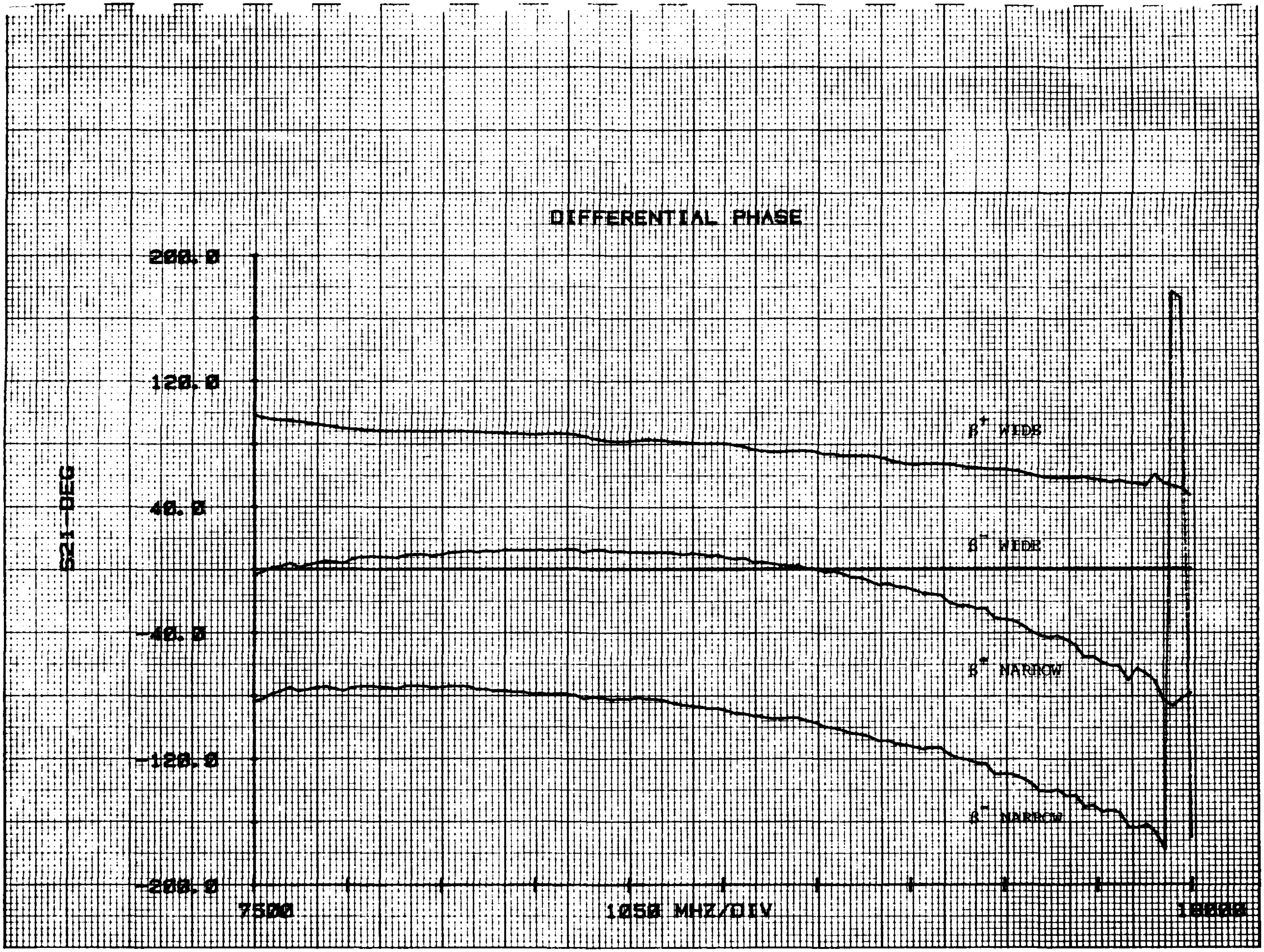

Figure 9. Differential Phase Shift

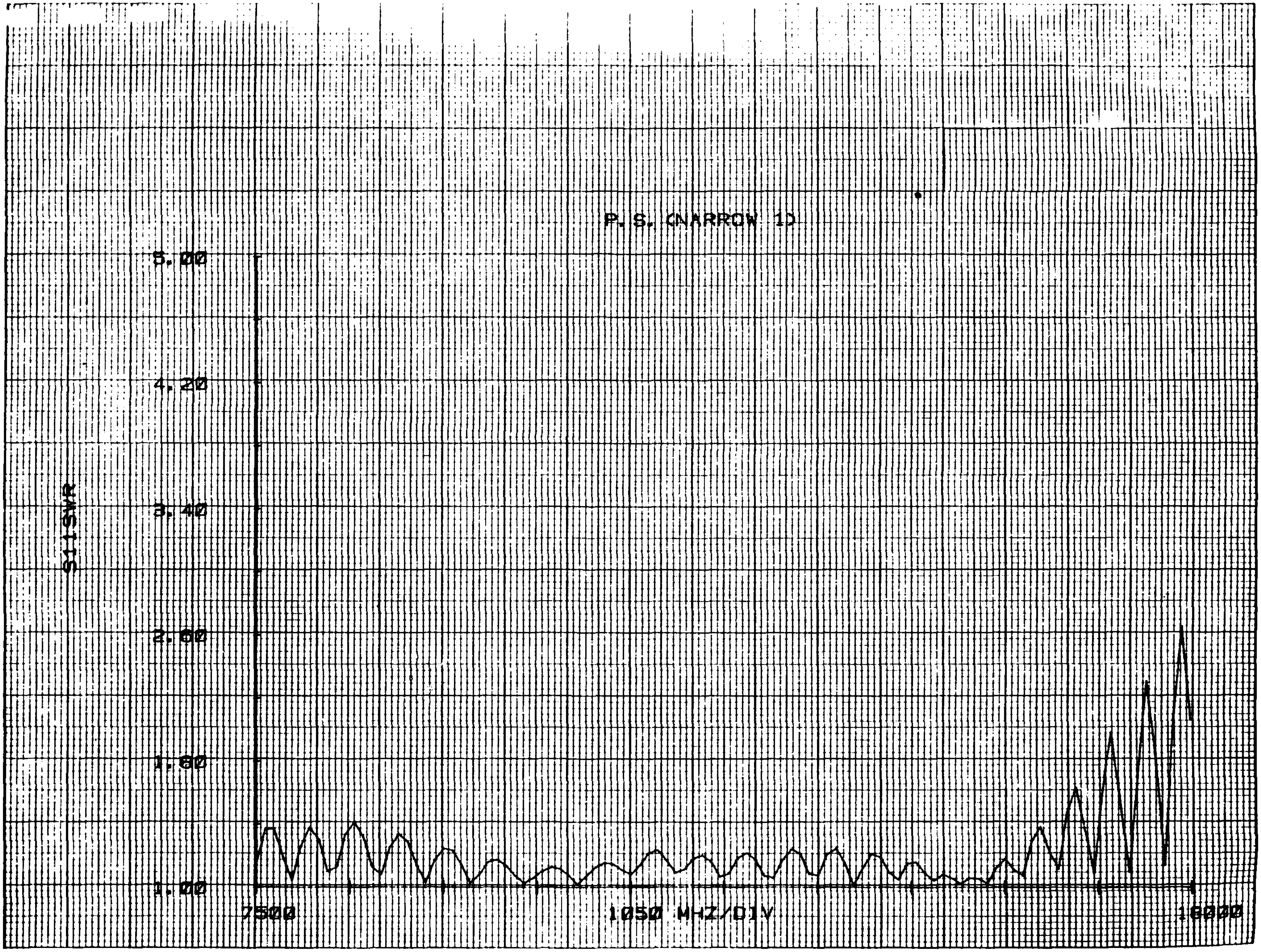

Figure 10. VSWR for Narrow Phase Shifter

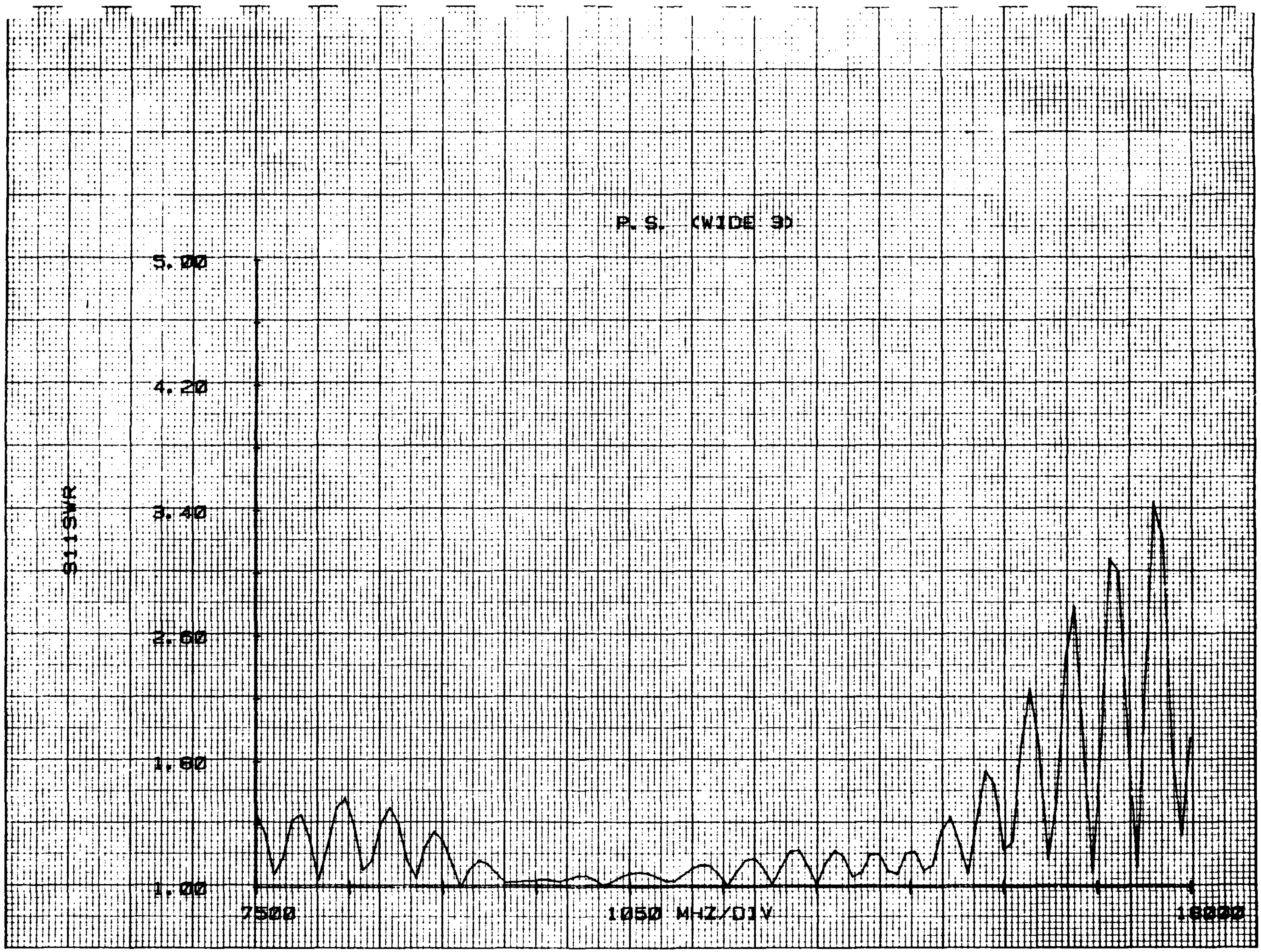

Figure 11. VSWR for Wide Phase Shifter

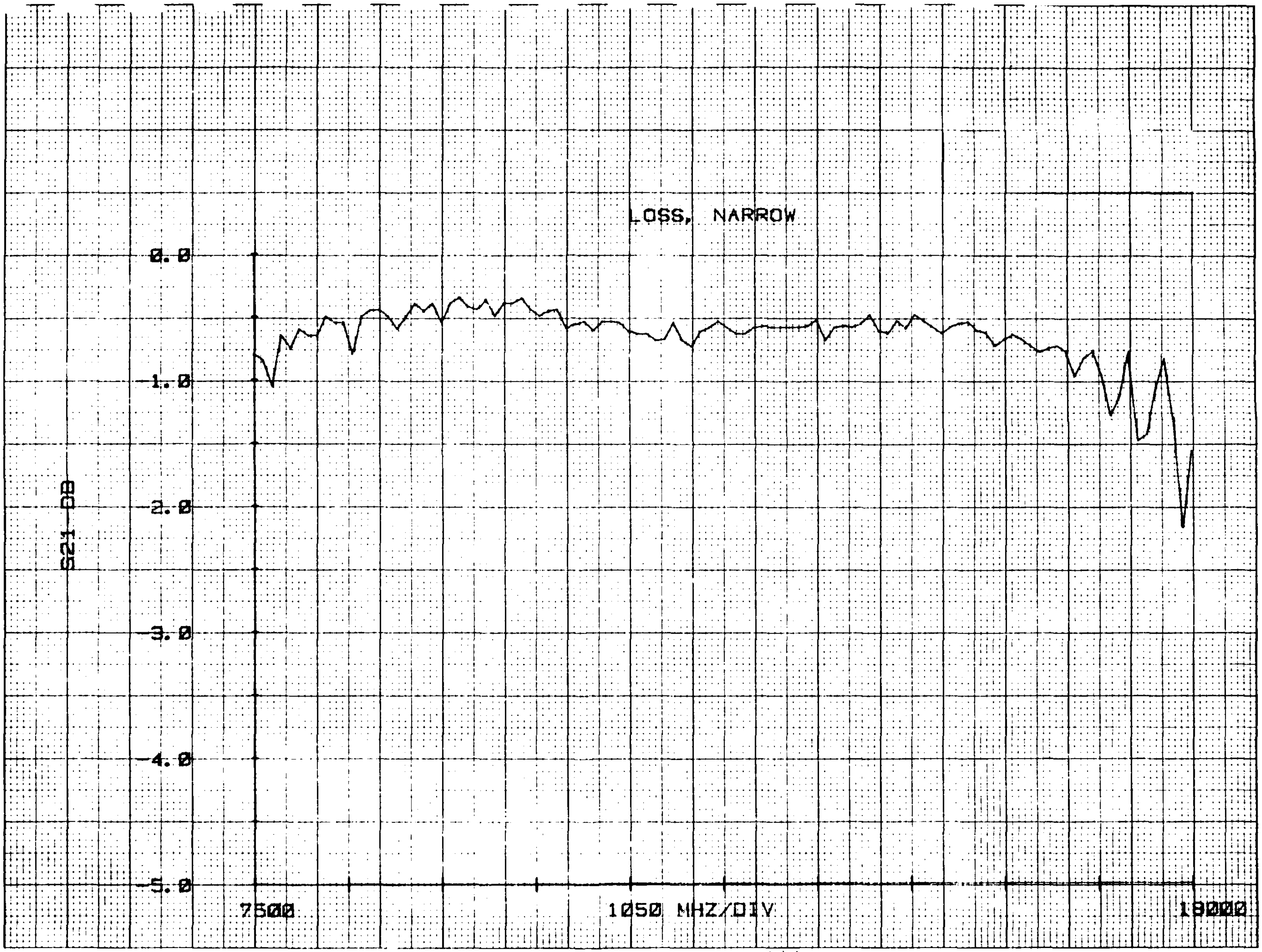

Figure 12. Insertion Loss for Narrow Phase Shifter

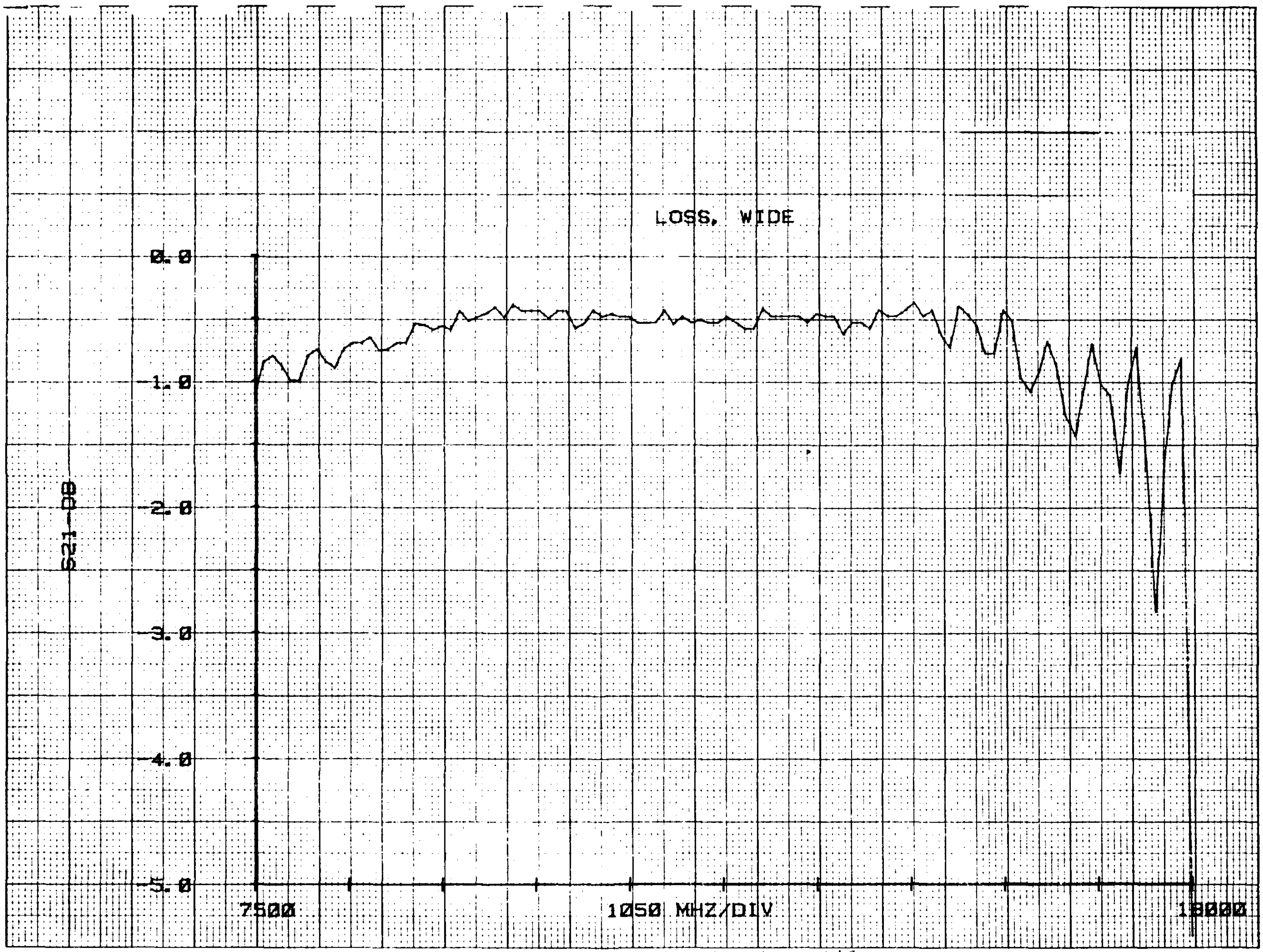

Figure 13. Insertion Loss for Wide Phase Shifter

5.0 MAGIC TEE

5.1 General Considerations

The major effort associated with the design of the hybrid magic tee is the impedance matching at the junction over the intended bandwidth. Methods of matching the junction include the use of reactive elements at the junction cavity, and transformers between the flanges of each arm and the actual junction at the cavity wall for each arm. In addition to matching problem, there are other considerations such as dissipated losses, phase balance, and power handling capacity. To minimize dissipated losses, it is desirable to avoid the use of dielectric materials, bonding agents or screws inside the waveguide cavity. Phase balance can be obtained as long as physical symmetry is maintained. In terms of power handling capacity, it is desirable to avoid sharp capacitive obstacles or low height construction in the waveguide.

5.2 Computer Analysis

In an attempt to study and design magic tee using double ridge waveguide, a computer program was written to find cutoff frequencies and characteristic impedance of double ridge waveguide. Cross-sectional shape of double ridge waveguide and its equivalent circuit representation is shown in Figure 14 and equations used for computation are summarized below without derivation.

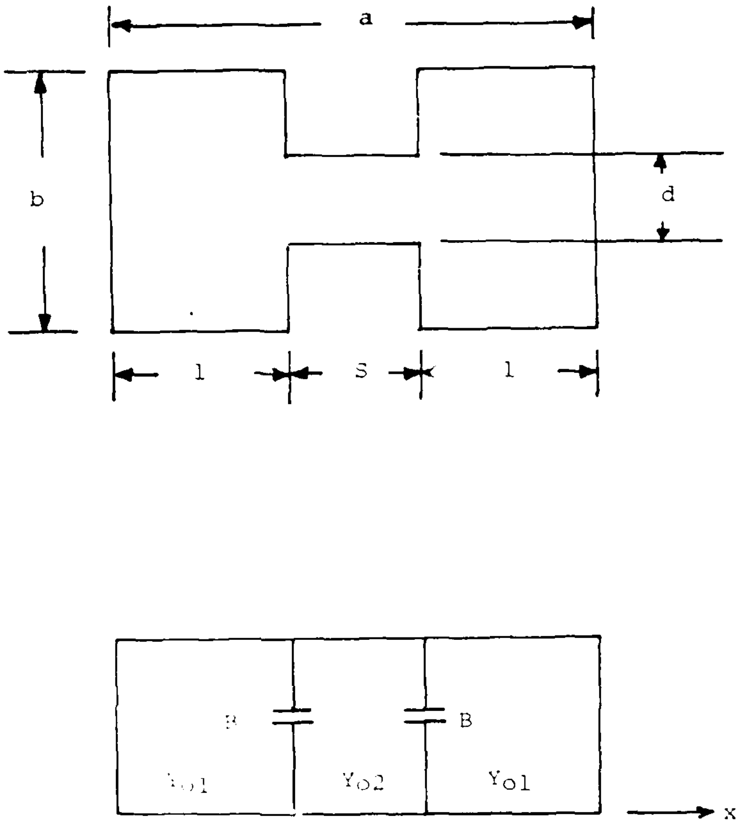

Figure 14. Double Ridge Waveguide Cross-Section and Its Equivalent Circuit Representation

(Original derivation of these equations can be found in Reference 3, 4, 5.)

The equations which govern the cutoff conditions of the TE_{no} type of modes are given by:

$$\cot k_x l - \frac{b}{d} \tan k_x s/2 - B/Y_{o1} = 0 \qquad (1)$$

$$\cot k_x l + \frac{b}{d} \cot k_x s/2 - B/Y_{o1} = 0 \qquad (2)$$

Equation (1) applies to the odd TE_{no} modes and (2) applies to the even TE_{no} modes. k_x is the propagation constant in the x direction at the cutoff and is given by $k_x = 2\pi/\lambda_c$. The characteristic admittances in the transverse direction (x-direction) Y_{o1} and Y_{o2} are defined as:

$$Y_{o1} = \frac{k_x}{\omega\mu} \frac{1}{b} \qquad Y_{o2} = \frac{k_x}{\omega\mu} \frac{1}{d}$$

(3) S.B. Cohn, "Properties of Ridge Waveguide", Proc. IRE, Vol. 35, pp. 783-788; August, 1947.

(4) T.G. Mihran, "Closed and Open-Ridge Waveguide", Proc. IRE, Vol. 37, pp. 640-644; June, 1949.

(5) S. Hopfer, "The Design of Ridge Waveguides", IRE. Trans., Vol. MTT-3, pp. 20-29; October, 1955

The value of the normalized susceptance term B/Y_{o1}, which represents the effect of the step discontinuity, can be obtained from Waveguide Handbook[2].

Employing power-voltage impedance definition, the characteristic impedance at infinite frequency for the TE_{10} mode is given by:

$$Z_{pv}^{\infty} = \frac{2 * 120\pi^2}{2\pi \dfrac{C_d}{\varepsilon_o} \cos^2\theta_2 + \lambda_c \left[\dfrac{\theta_2}{d} + \dfrac{\sin 2\theta_2}{2d} + \dfrac{2\cos^2\theta_2}{b * \sin^2\theta_2} \left[\dfrac{\theta_1}{2} - \dfrac{\sin 2\theta_1}{4} \right] \right]} \tag{3}$$

where λ_c is cutoff wavelength of ridge waveguide.

$$\theta_1 = \frac{\pi(a-s)}{\lambda_c}$$

$$\theta_2 = \frac{\pi s}{\lambda_c}$$

$$C_d = \frac{\varepsilon_o}{\pi} \left[\frac{\left(\frac{d}{b}\right)^2 + 1}{\left(\frac{d}{b}\right)} \cosh^{-1} \left[\frac{1+(d/b)^2}{1-(d/b)^2} \right] - 2 * \ln \frac{4(d/b)}{1-(d/b)^2} \right]$$

The characteristic impedance at any frequency f is obtained by:

$$Z_{pv}(f) = \frac{\lambda_g}{\lambda} \times Z_{pv}^{\infty} = \frac{1}{\sqrt{1 - \left(\frac{f_c}{f}\right)^2}} \qquad (4)$$

5.3 Magic Tee Design

Initially, magic tee was designed based on intuitive reasoning. At the cavity junction impedance ratio of H-arm, colinear arm, and E-arm is assumed to be 1:2:4. Then Chebyshev type multisection quarterwave transformer between flanges of each arm (WRD750D24) and cavity junction of each arm were computed using equation (4). Cutoff frequencies of TE_{10} and TE_{20} mode at the junction were also computed. Based on the computed results, two sets of brassboard magic tees were made. Brassboard was chosen so that additional metal could be soldered in place whenever design modification is necessary. Figure 15 shows simplified sketch of the magic tee. For the purpose of evaluation of characteristic impedance of double ridge waveguide and verification of the theoretical result, each magic tee was made in three separate parts.

Part 1: H-Arm

Designed with four section step-down quarterwave transformer between WRD750D24 and H-arm junction.

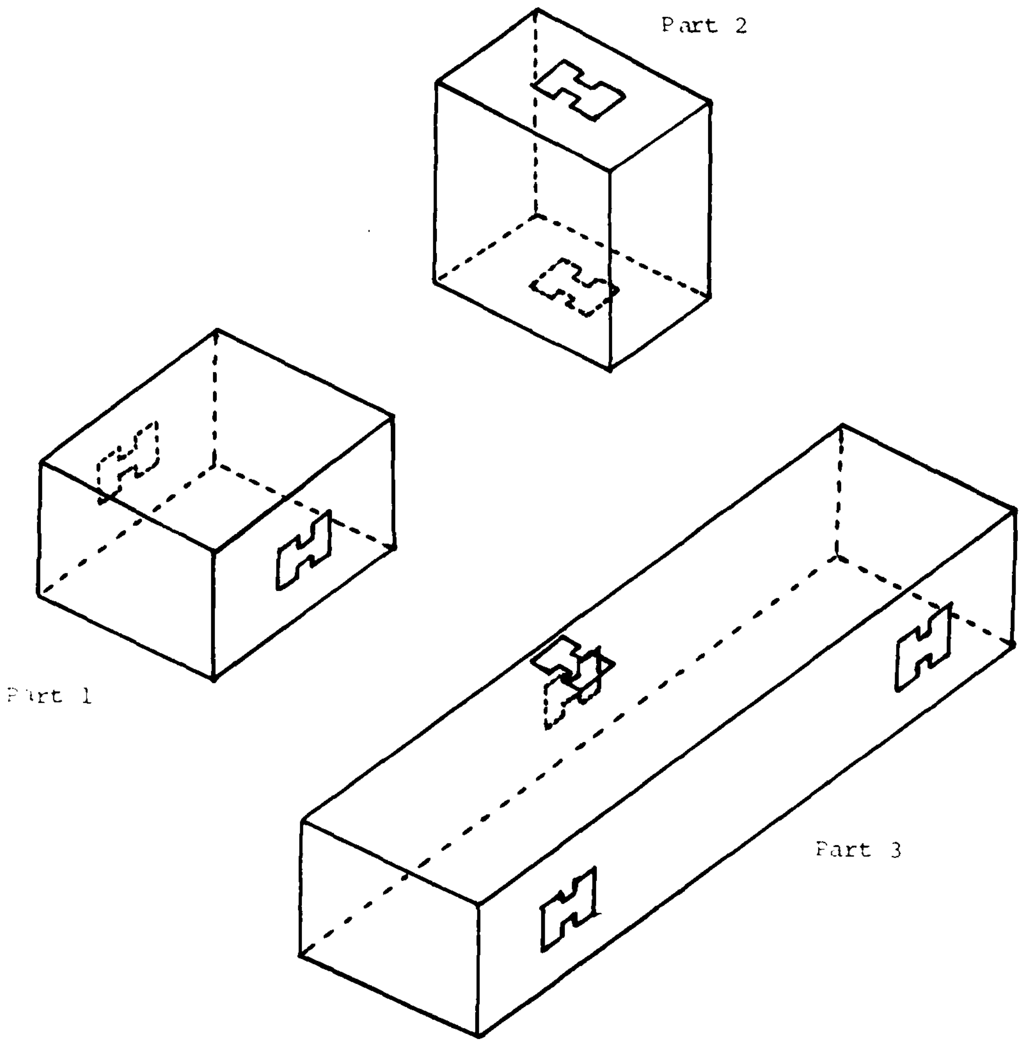

Figure 15. Brassboard Magic Tee

Part 2: E-Arm

Designed with 3 section step-up quarterwave transformer between WRD750D24 and E-arm junction.

Part 3: Colinear Arm Including Junction Cavity

Designed with 4 section step-down quarterwave transformer between WRD750D24 and colinear arm junction.

Since Part 1 and Part 2 of the magic tee do not include junction cavity, these parts were used to verify computed characteristic impedance of the double ridge waveguide. VSWR of H-arm (two H-arm in back to back configuration) was measured and Smith Plot of the measured VSWR is shown in Figure 16. Smith Plot of VSWR for the same configuration was computed using transmission line equation employing characteristic impedance given by Equation (4). Computed results, shown in Figure 17, were in good agreement with experimental results.

Due to the difficulties of transmission line model including junction cavity, no attempt has been made to analyze magic tee as a whole theoretically. Instead, it was intended to find optimum matching structure experimentally by using reactive element at the junction cavity. The effect of reactive element can be measured at the flanges of each arm, and then these measured impedance can be transformed to cavity junction wall using transmission line equation. Based on these transformed impedance, necessary

NAME	TITLE	DWG. NO.
	H-Arm (BACK TO BACK)	DATE
SMITH CHART FORM 82 SPR (2-49)	KAY ELECTRIC COMPANY, PINE BROOK, N.J. ©1949 PRINTED IN U.S.A.	

IMPEDANCE OR ADMITTANCE COORDINATES

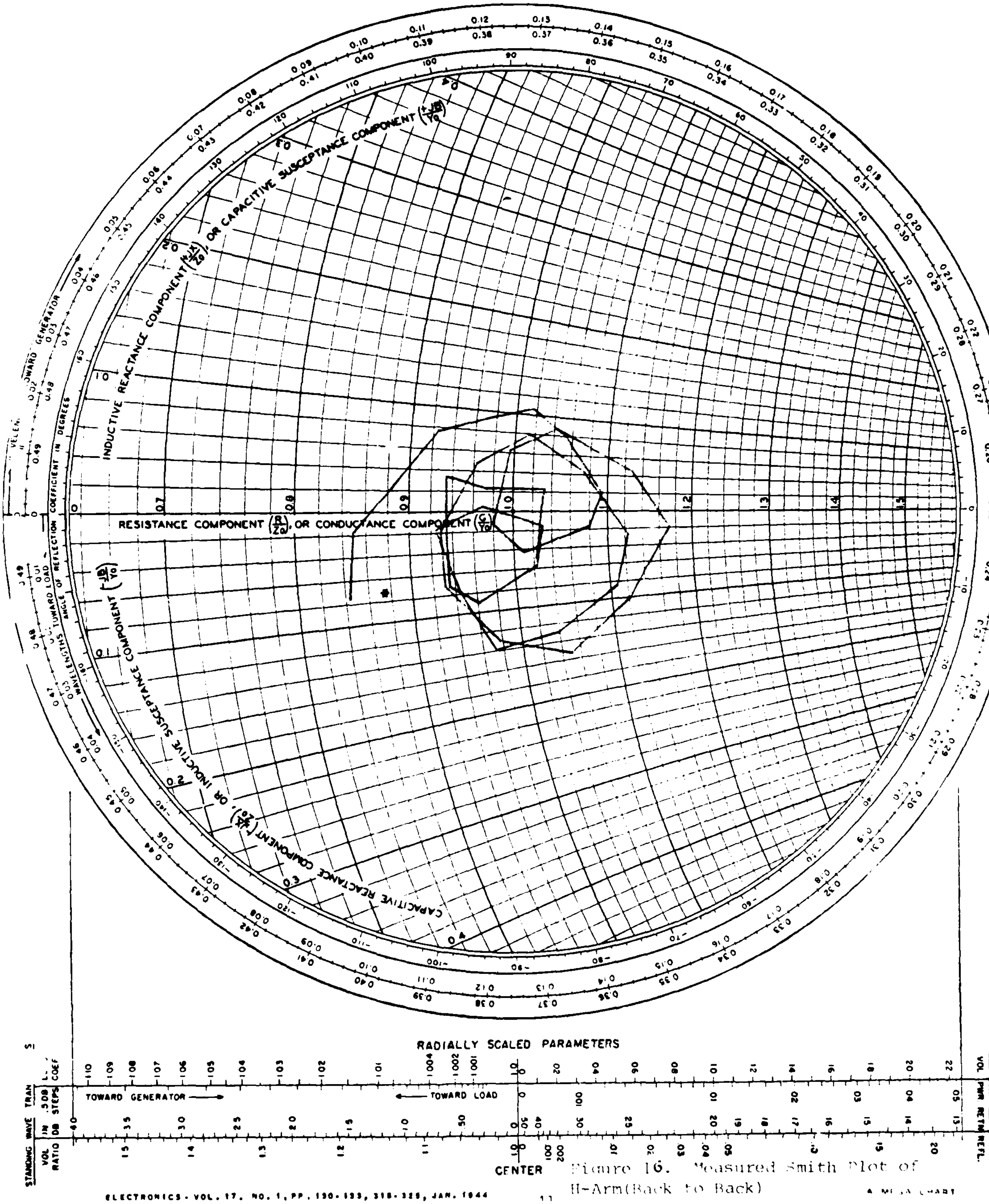

Figure 16. Measured Smith Plot of H-Arm(Back to Back)

ELECTRONICS - VOL. 17, NO. 1, PP. 130-133, 318-325, JAN. 1944

A MEGA CHART

NAME	TITLE	DWG. NO.
SMITH CHART FORM 82 SPR (2-49)	KAY ELECTRIC COMPANY, PINE BROOK, N.J. ©1949 PRINTED IN U.S.A.	DATE

IMPEDANCE OR ADMITTANCE COORDINATES

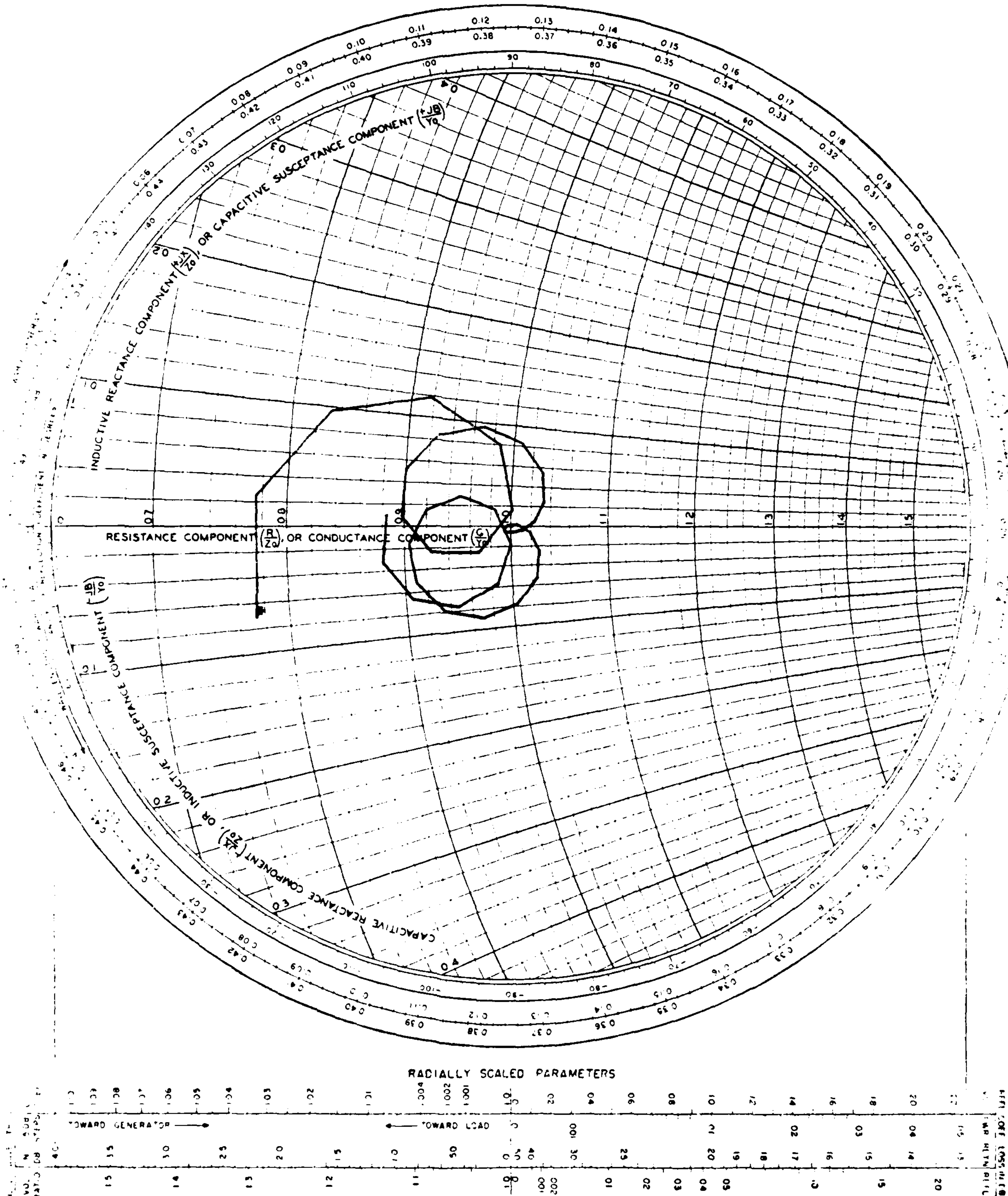

Figure 17. Computed Smith Plot of H-Arm (Back to Back)

modification can be made. This method requires iterative process of microwave measurement, engineering analysis, and modification. However, this method has not been pursued due to the time constraint. Therefore, magic tees designed by Raytheon for previous projects were used for final assembly of circulator. These magic tees were designed for frequency range between 8 to 18 GHz. Performance data of magic tees are shown in Figures 18 through 25.

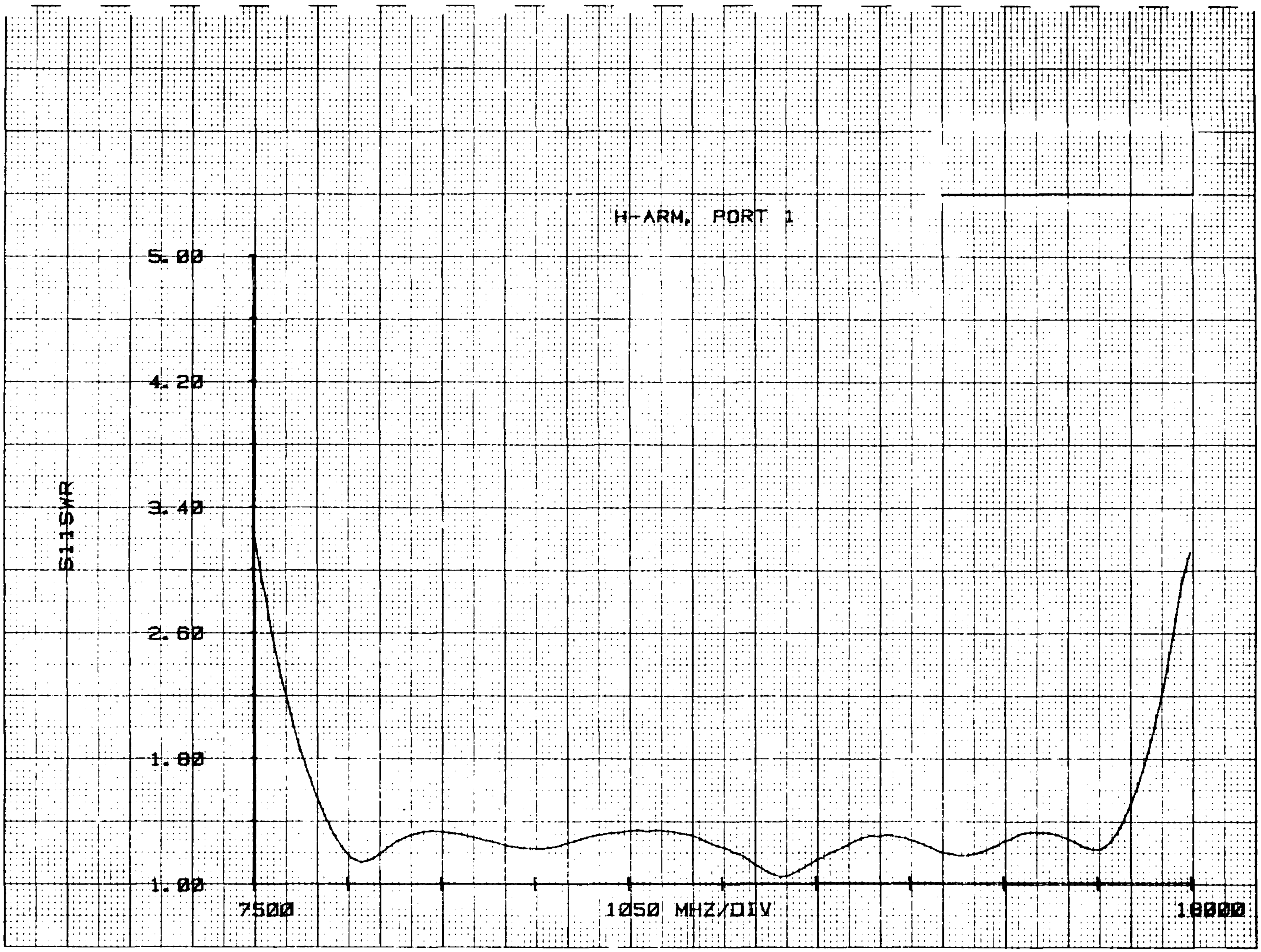

Figure 18. VSWR of H-Arm, Tee 1

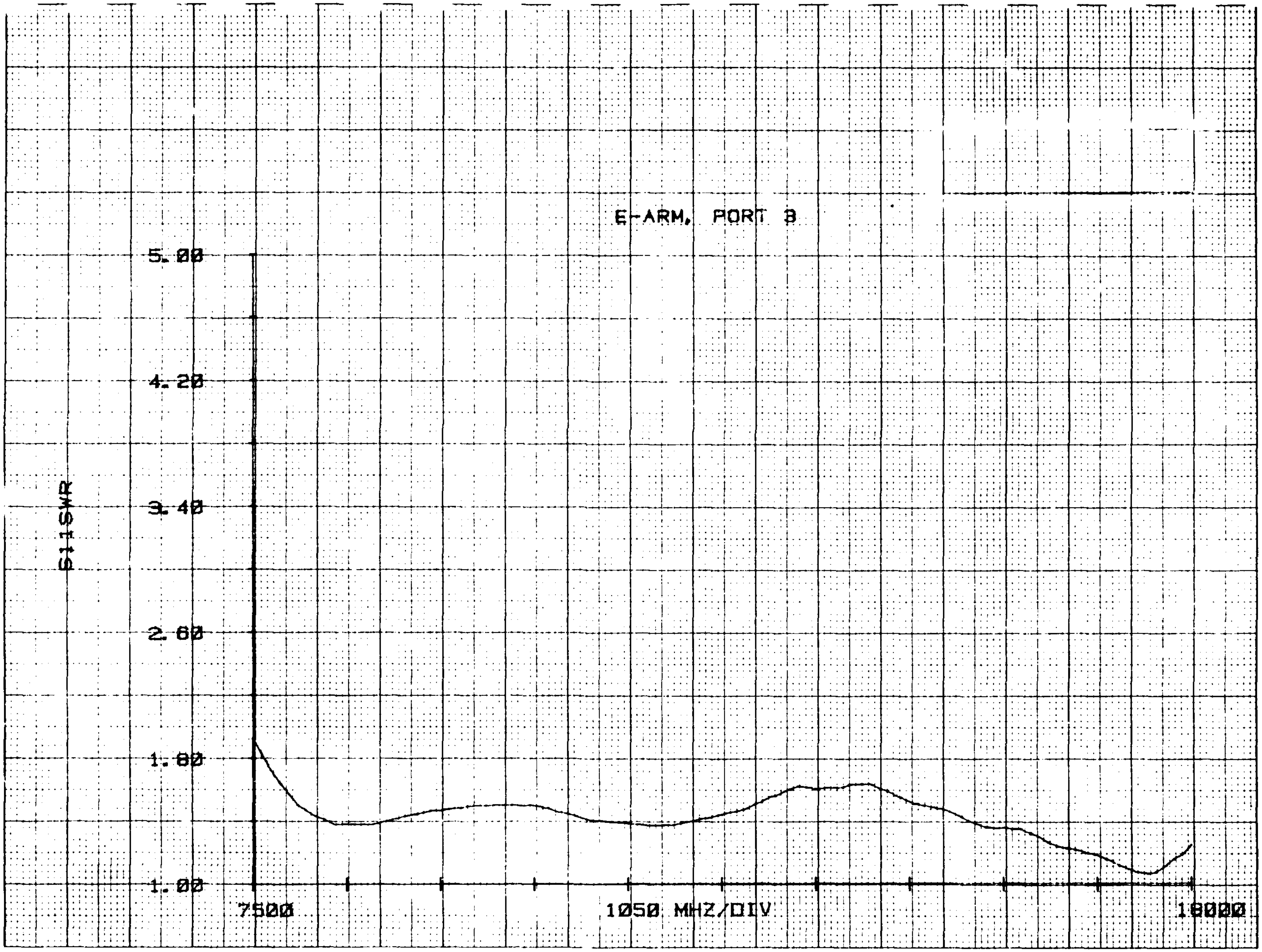

Figure 19. VSWR of E-Arm, Tee 1

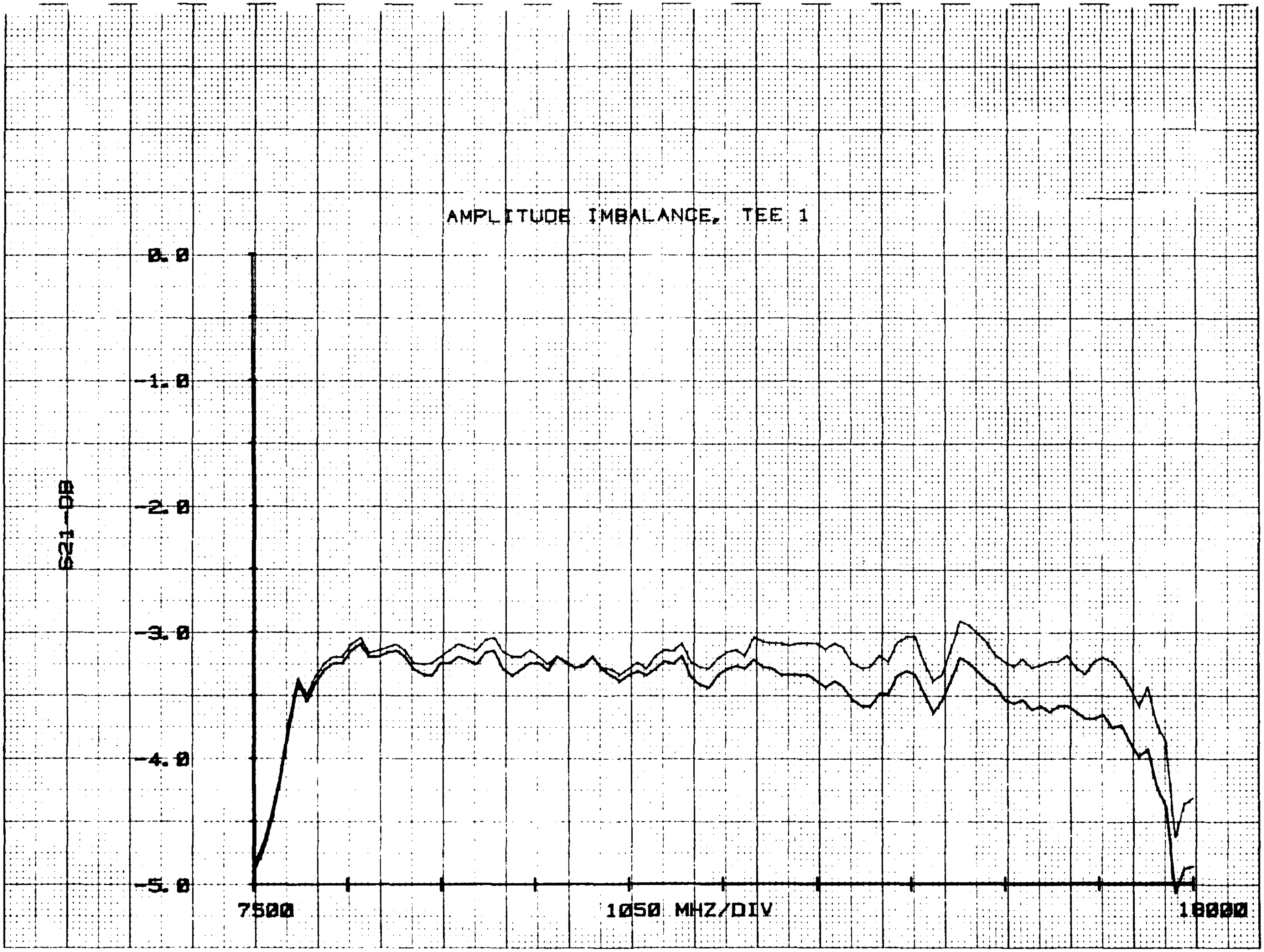

Figure 20. Amplitude Imbalance of Tee 1

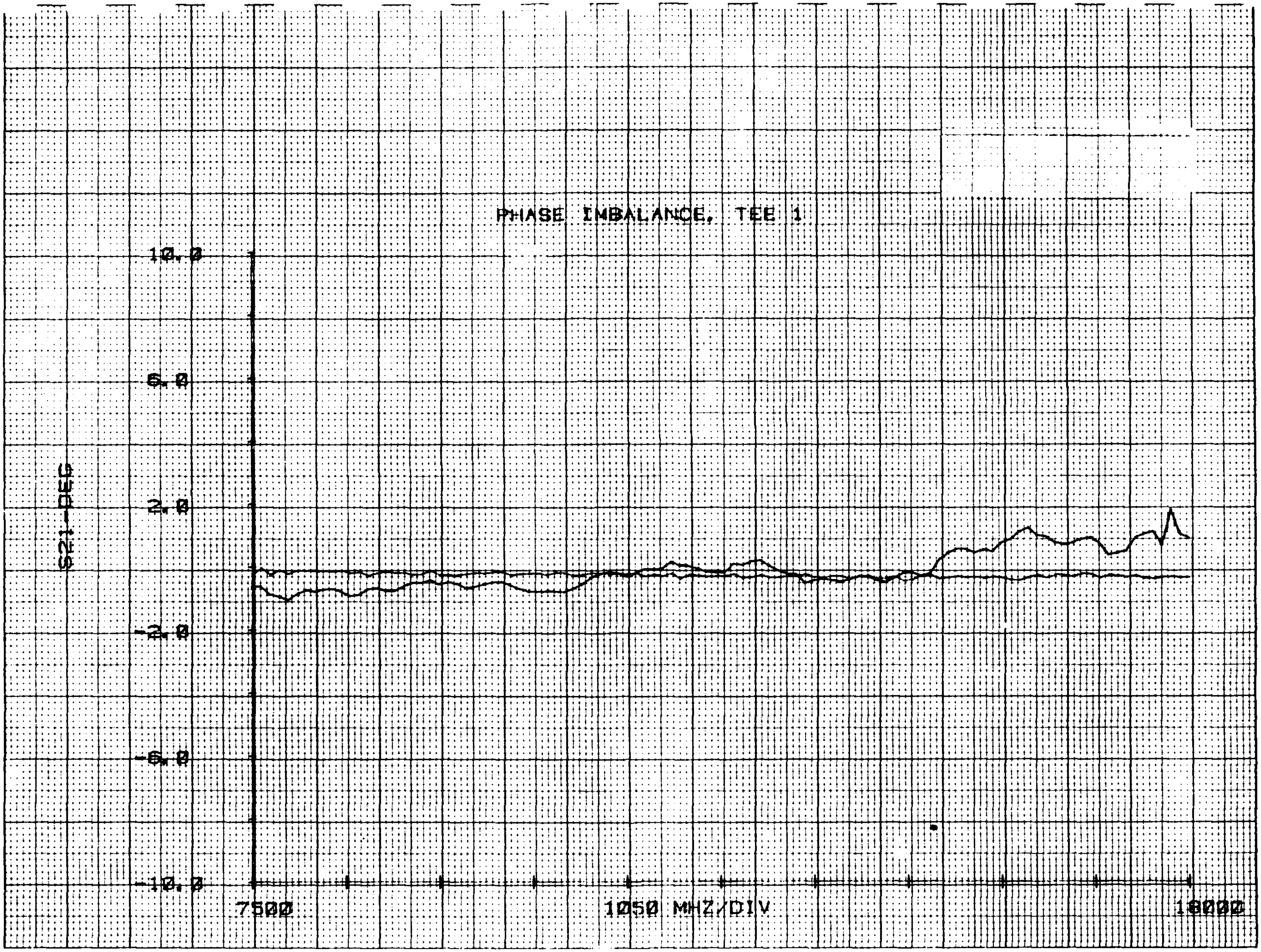

Figure 21. Phase Imbalance of Tee 1

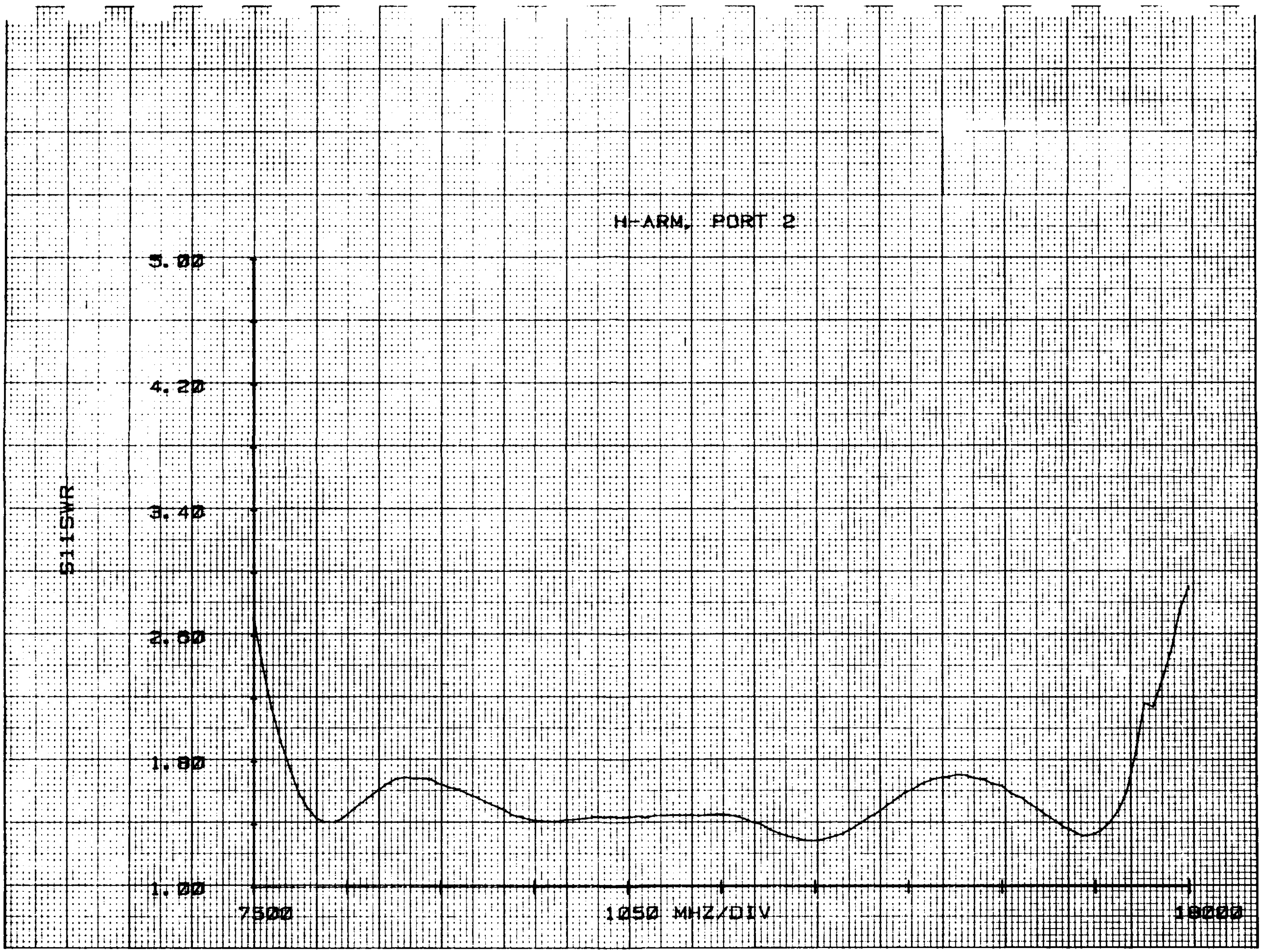

Figure 22. VSWR of H-Arm, Tee 2

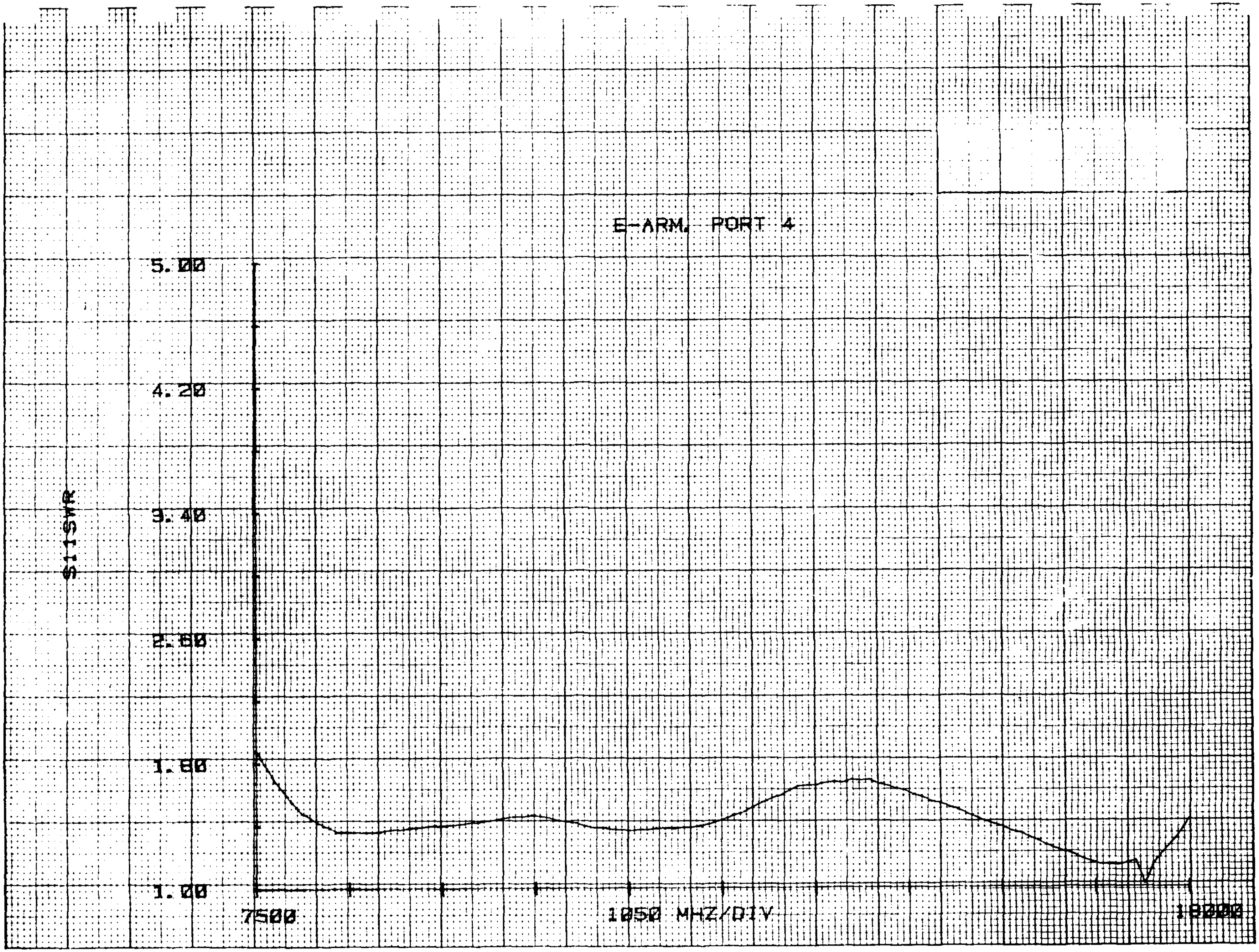

Figure 23. VSWR of E-Arm, Tee 2

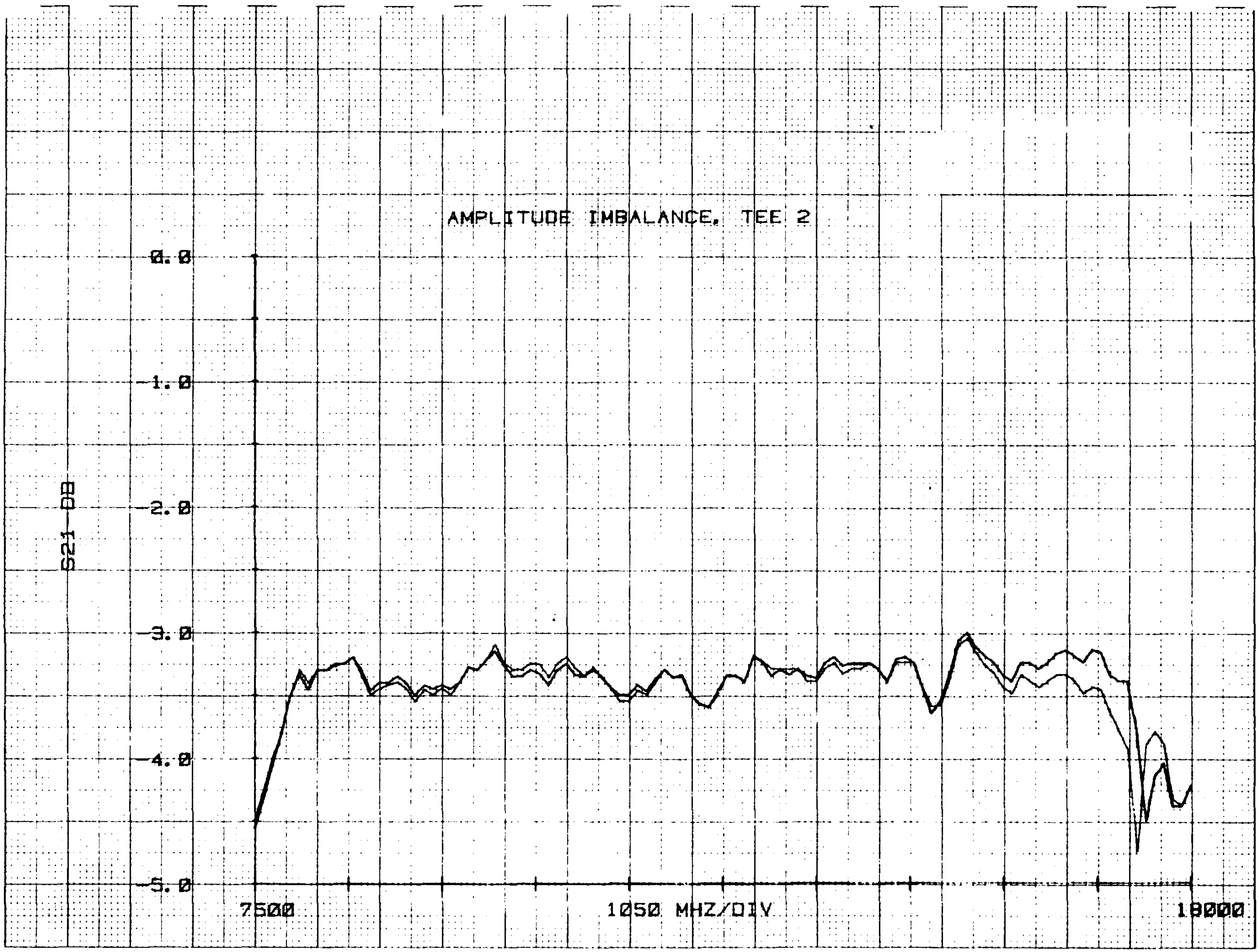

Figure 34. Amplitude Imbalance of Tee 2

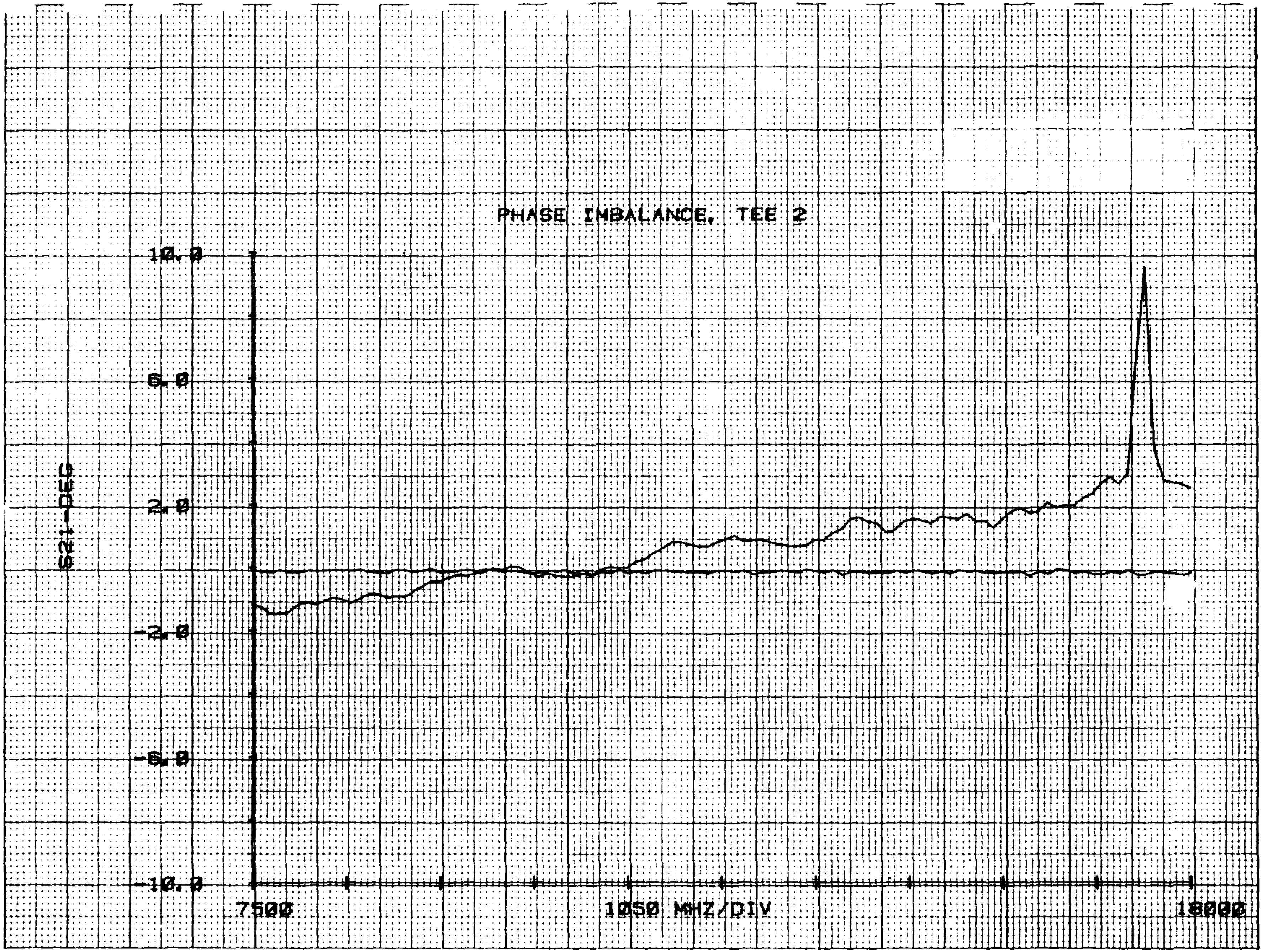

Figure 25. Phase Imbalance of Tee 2

6.0 HIGH POWER

High power measurement has not been performed for the circulator assembled. According to estimation based upon available informations, circulator would require pressurization and efficient cooling for safe operation at the specified high power level.

6.1 Peak Power

6.1.1 Magic Tee

Magic tee used for circulator assembly include capacitive obstacles for optimum matching. In order to guarantee safe operation at the specified power level, pressurization of waveguide would be necessary. Pressurization windows for the specified power level do not exist at this time. Microwave Research Corporation Model 270 is rated at 10 KW peak/600 watts average for a VSWR of <1.1.1 and loss of <0.1 dB. Microwave Development Labs have a unit under development. Further development will be necessary if the desired power levels of 20 KW peak/1 KW average are to be met.

6.1.2 Phase Shifter

There are two effects of concern in the phase shifter section, breakdown and nonlinearity. Nonlinearity is the increase in insertion loss above a certain peak power threshold. Ferrite material used for phase shifters design has been utilized previously for the similar frequency range with comparable geometry. To prevent peak power breakdown, air gap should be removed in bonding of dielectric rib.

6.2 Average Power

6.2.1 Magic Tee

The average power capability of the magic tees would be adequate if conduction cooling to liquid cooled phase shifters is used.

6.2.2 Phase Shifter

Since the phase tracking is essential for the operation of the circulator, efficient cooling of phase shifter is required to prevent phase change due to temperature variations. Liquid cooling with pressure drop of 10 psi would be adequate.

7.0 CIRCULATOR ASSEMBLY AND TEST DATA

Cross-sectional view of phase shifters for the circulator assembly is shown in Figure 26. Final data on circulator assembly are shown in Appendix A. WRD750D24 calibration standards were used in the calibration. The designation Port X-Y indicates that Port X was the input port while output signals were measured at Port Y.

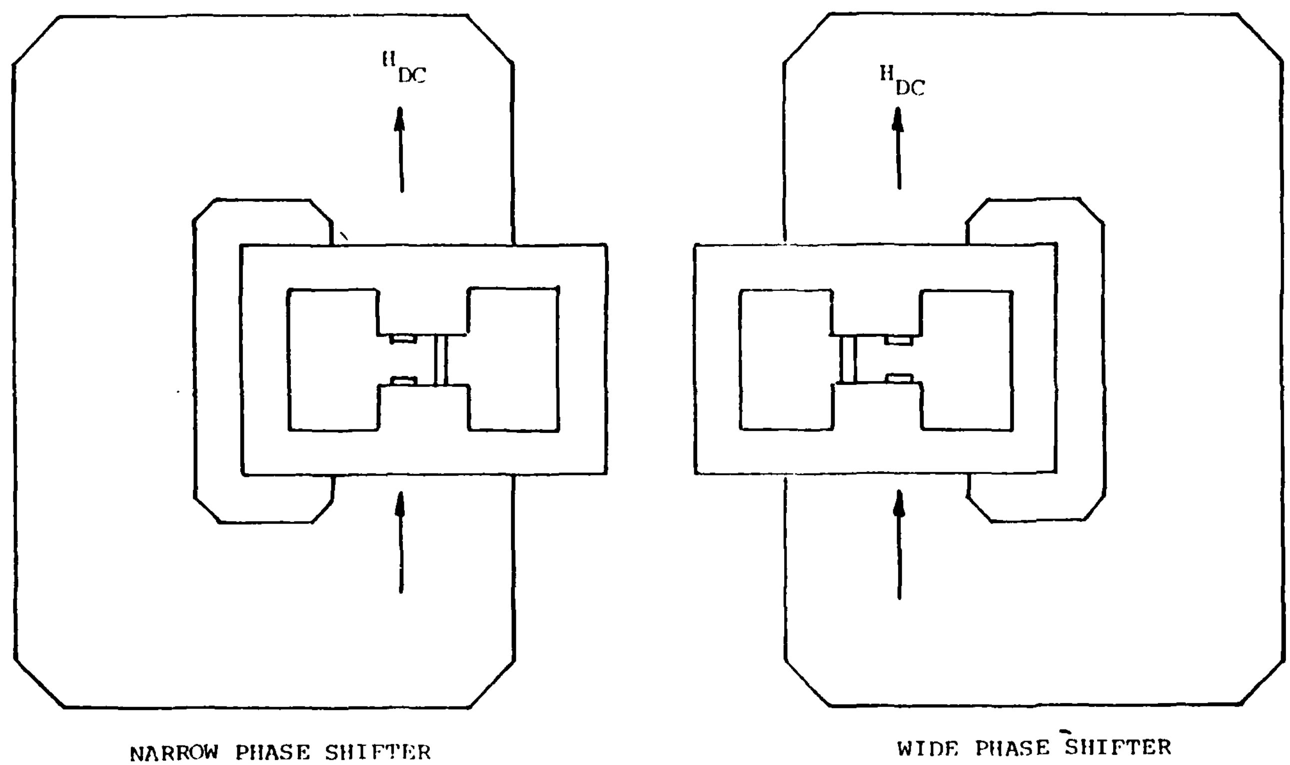

Figure 26. Cross-Sectional View of Phase Shifters for Circulator Assembly (Port 1 is Toward Viewer)

8.0 CONCLUDING REMARKS

Four port differential phase shift circulator under Contract No. N00173-80-C-0434 for Naval Research Laboratory has been built. For frequency range between 8 to 16 GHz, 11 dB minimum isolation, 1.8 dB maximum insertion loss, and maximum VSWR of 2:1 were achieved. Even though the performance of the circulator designed did not meet the originally intended specification, it has demonstrated, at least, the feasibility of building the broadband four port differential phase shift circulator.

APPENDIX A

PERFORMANCE DATA

RAYTHEON CKuH40 PORT 1-2

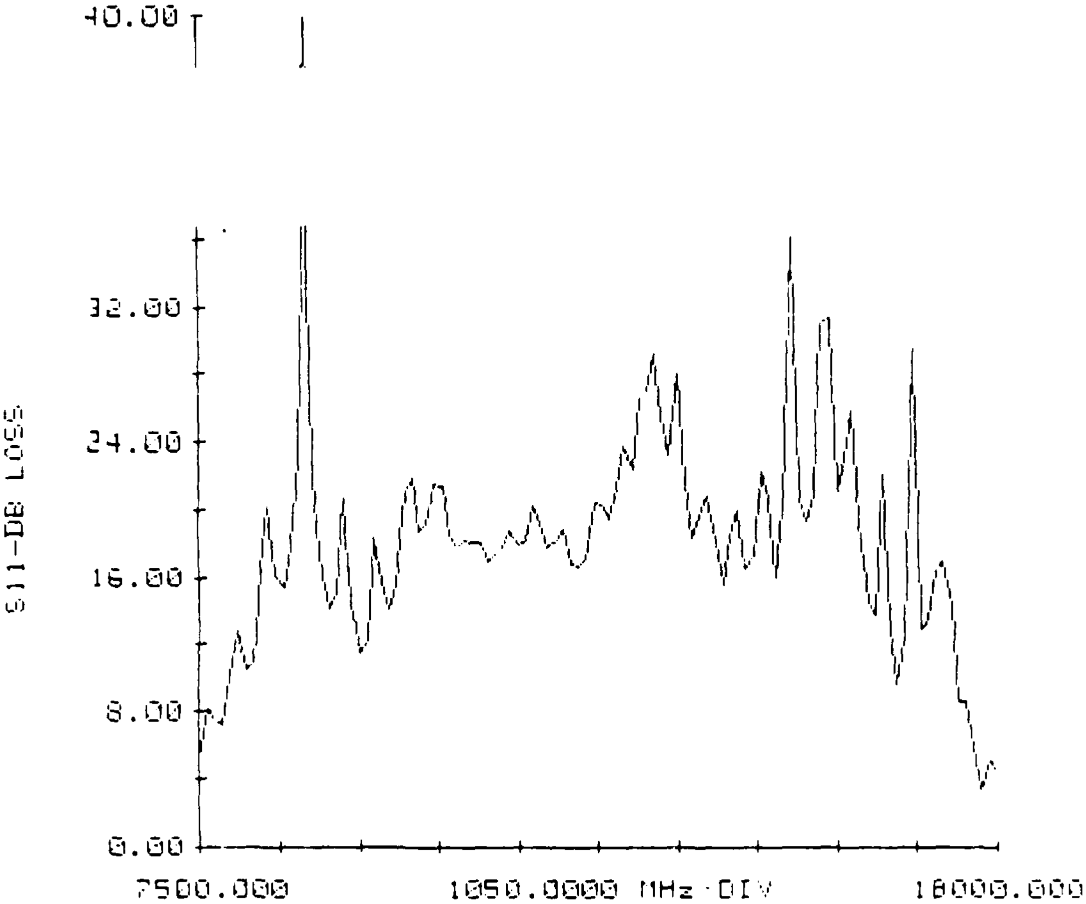

RAYTHEON CKuH40 PORT 1-2

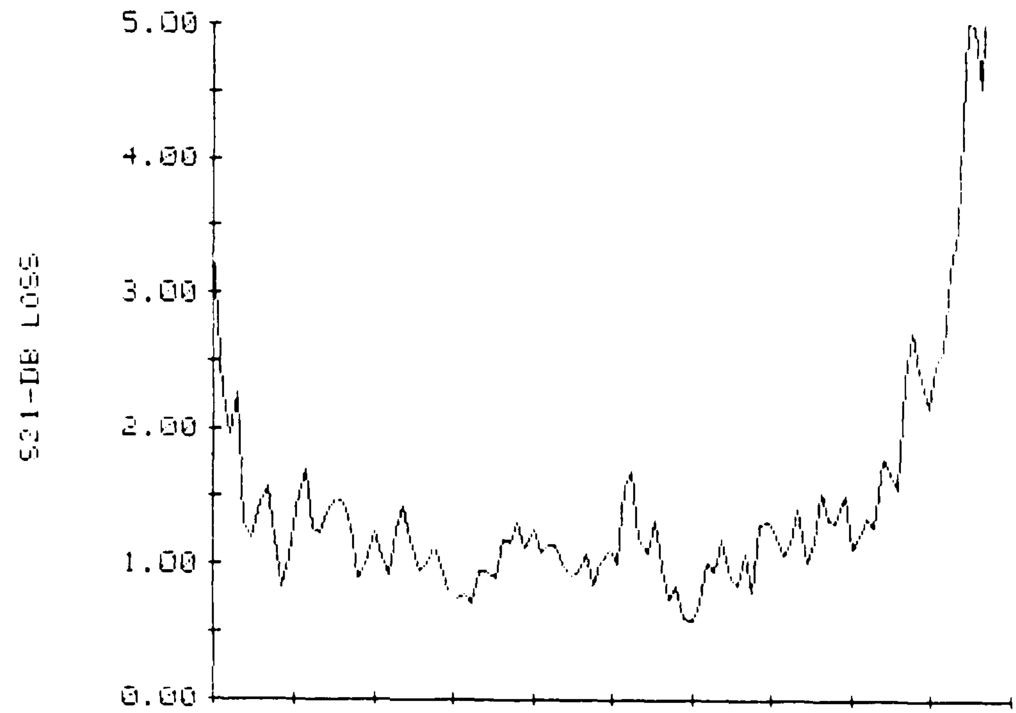

RAYTHEON CKuH40 PORT 1-3

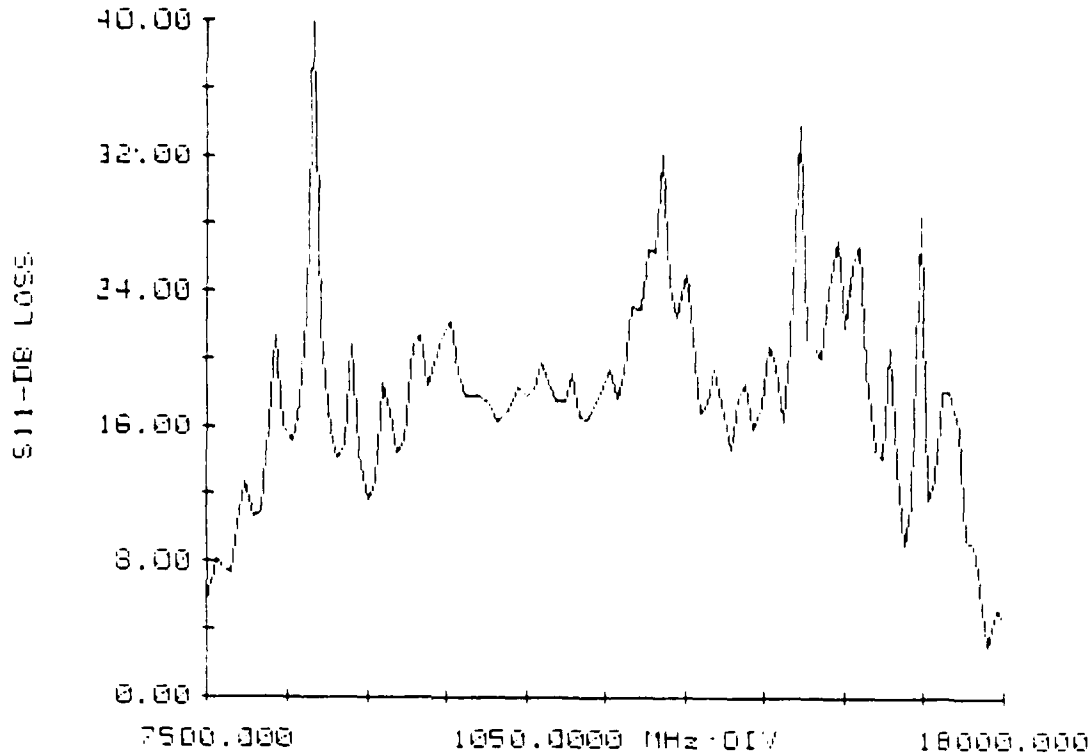

RAYTHEON CKuH40 PORT 1-3

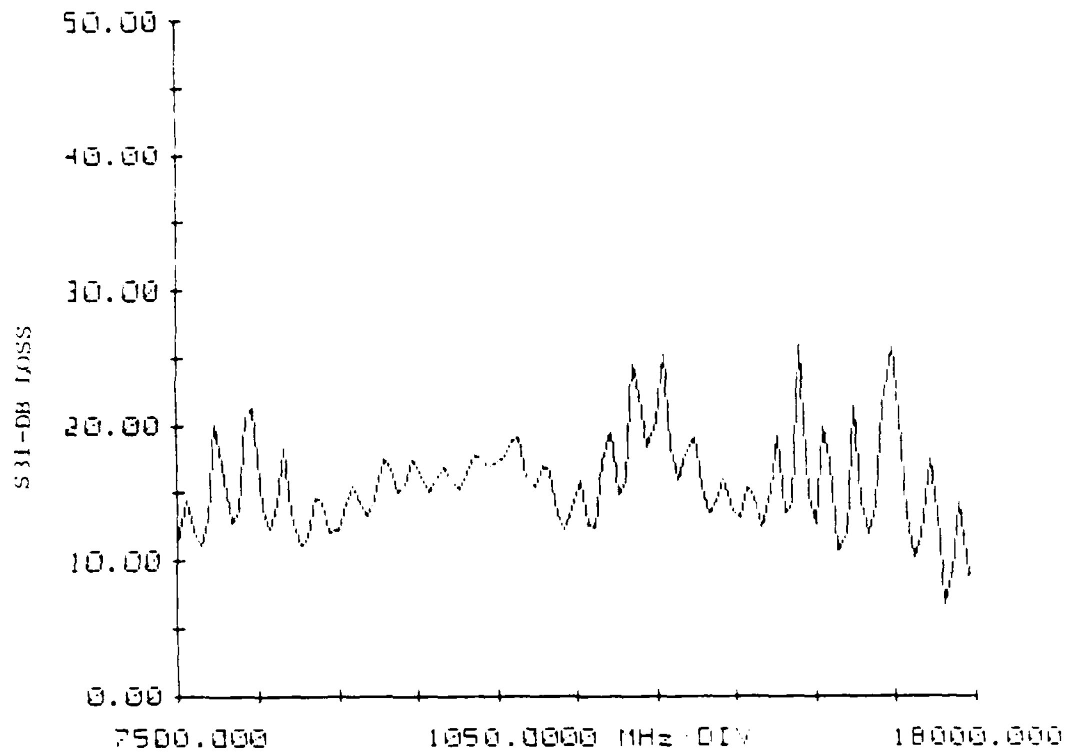

RAYTHEON CKuH40 PORT 1-4

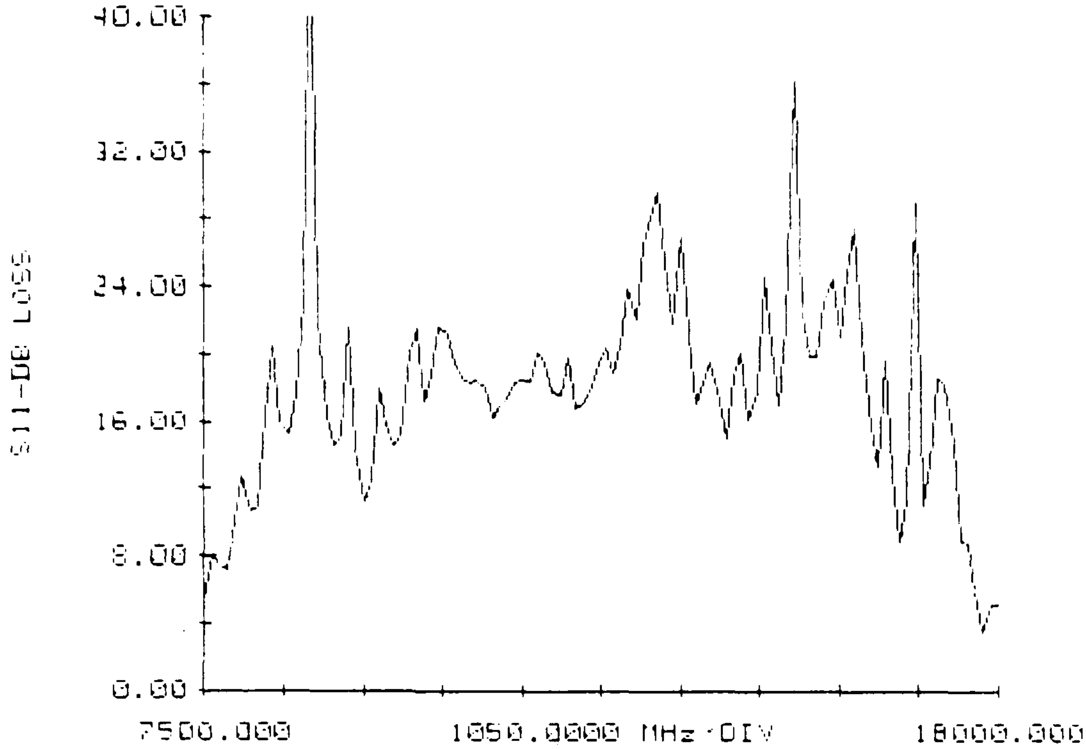

RAYTHEON CKuH40 PORT 1-4

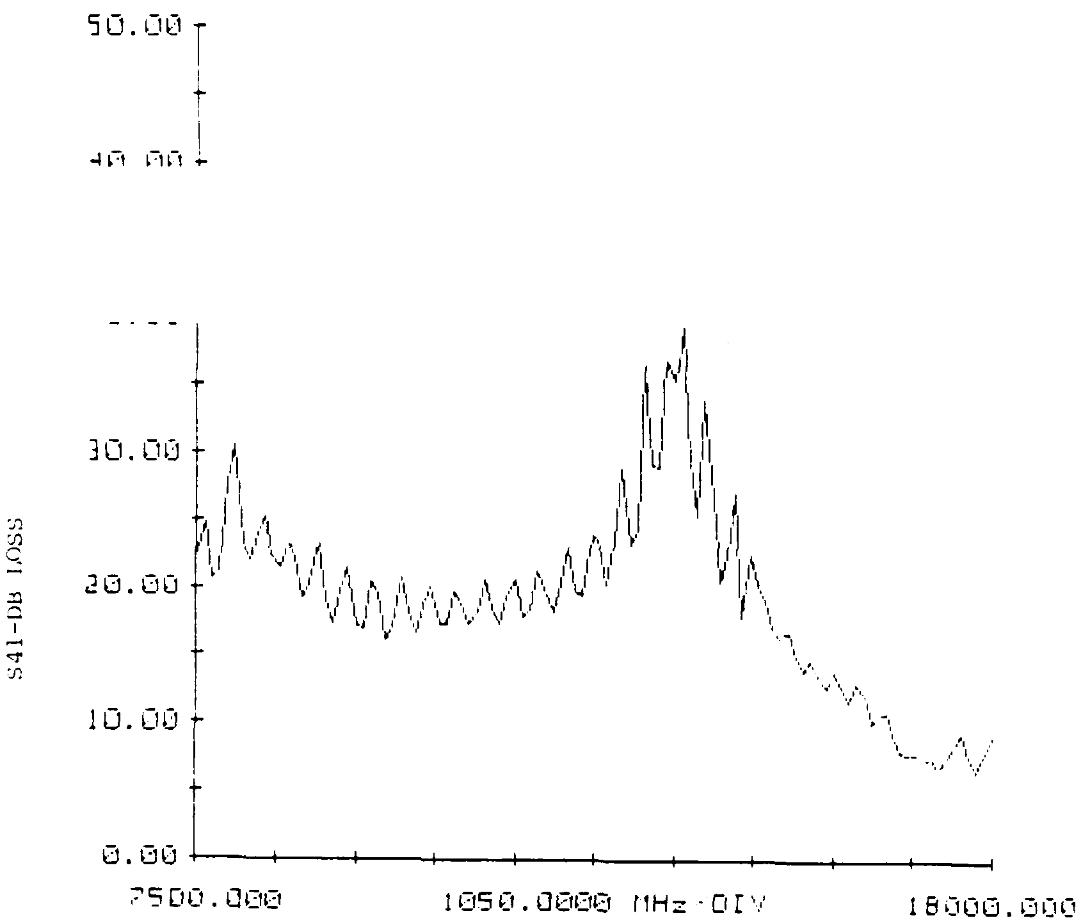

RAYTHEON CKuH40 PORT 2-1

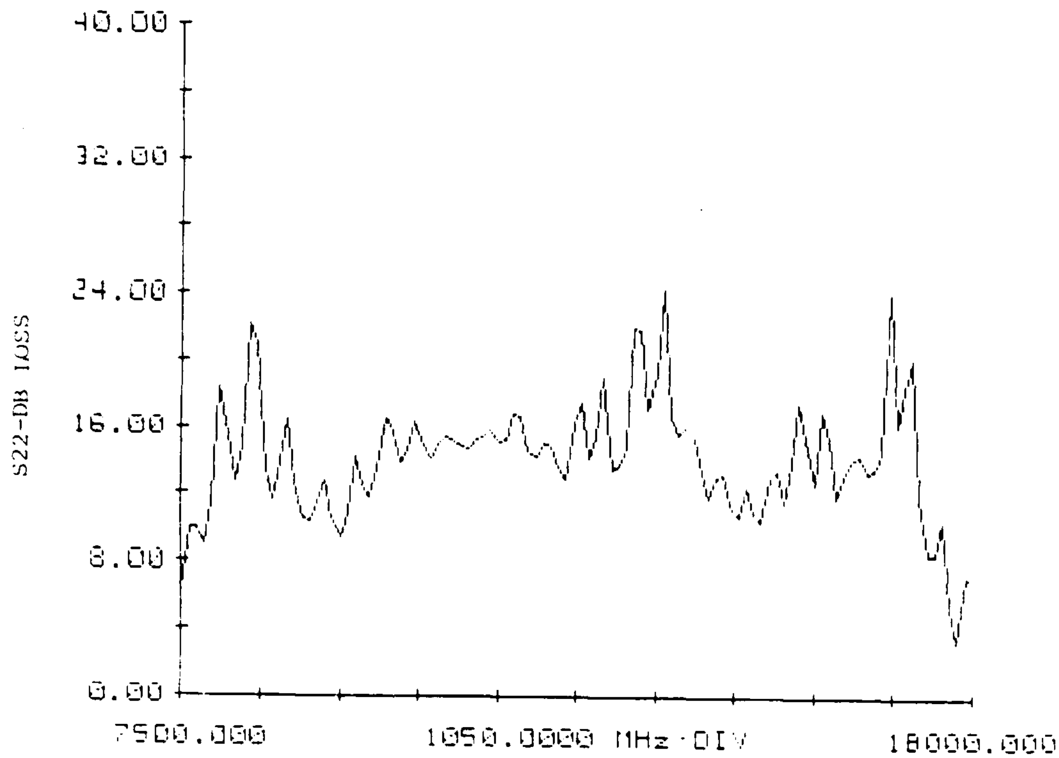

RAYTHEON CKuH40 PORT 2-1

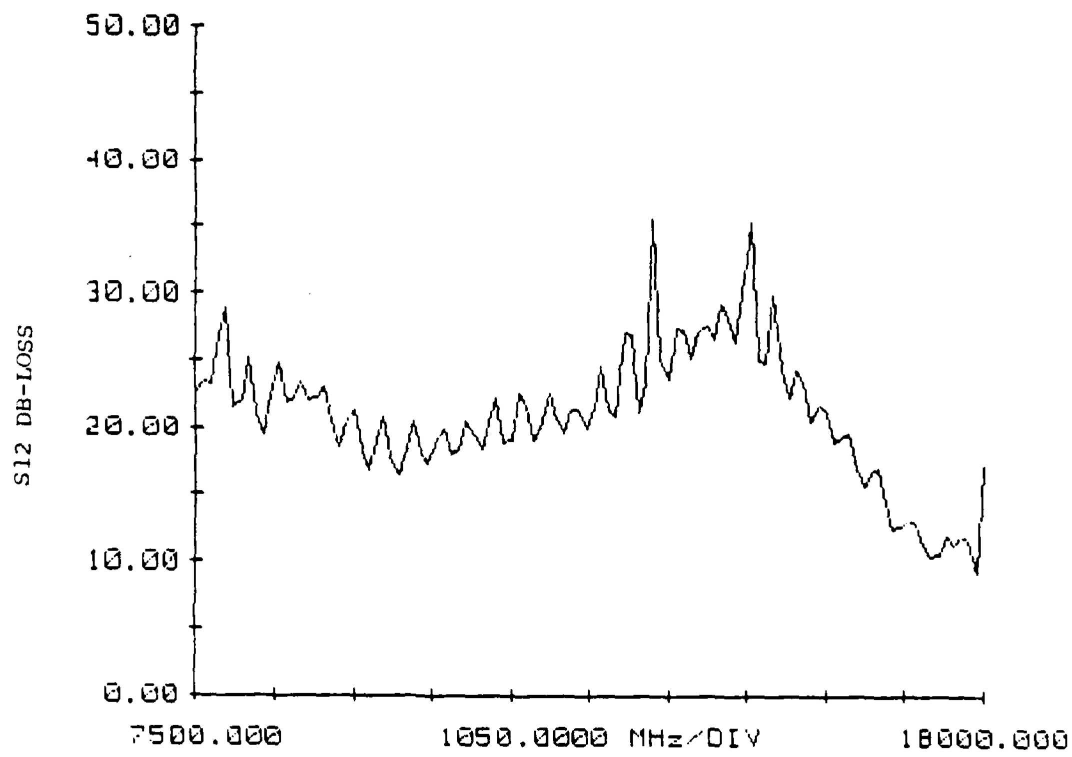

RAYTHEON CKuH40 PORT 2-3

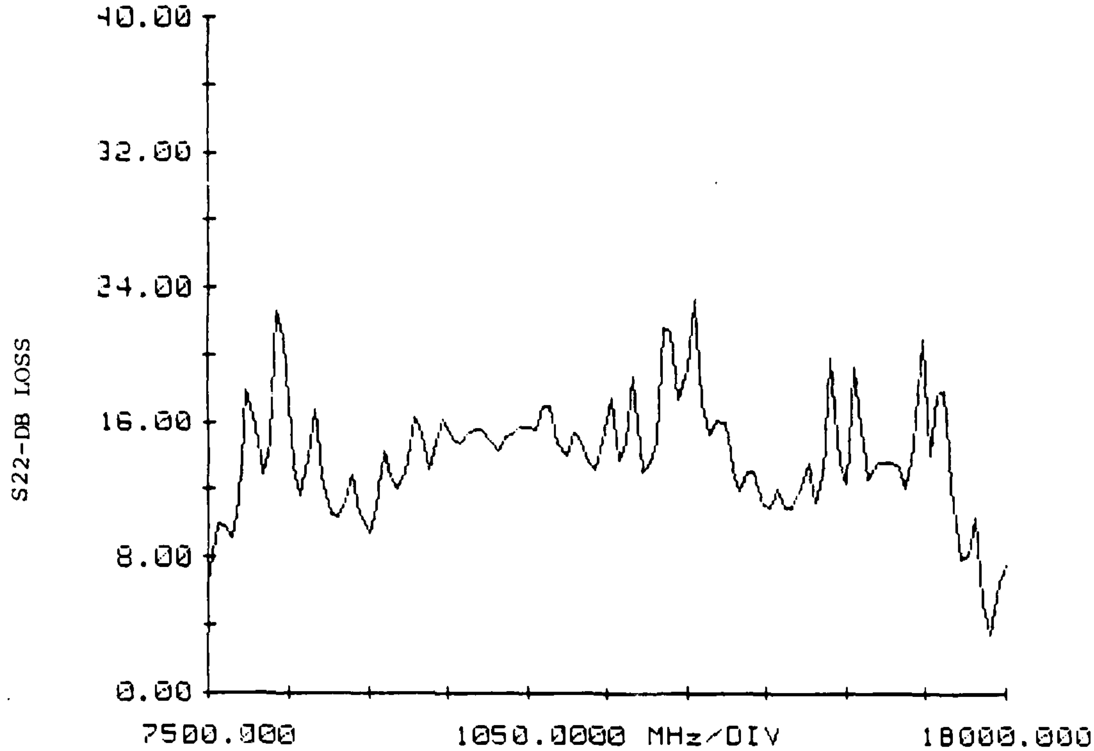

RAYTHEON CKuH40 PORT 2-3

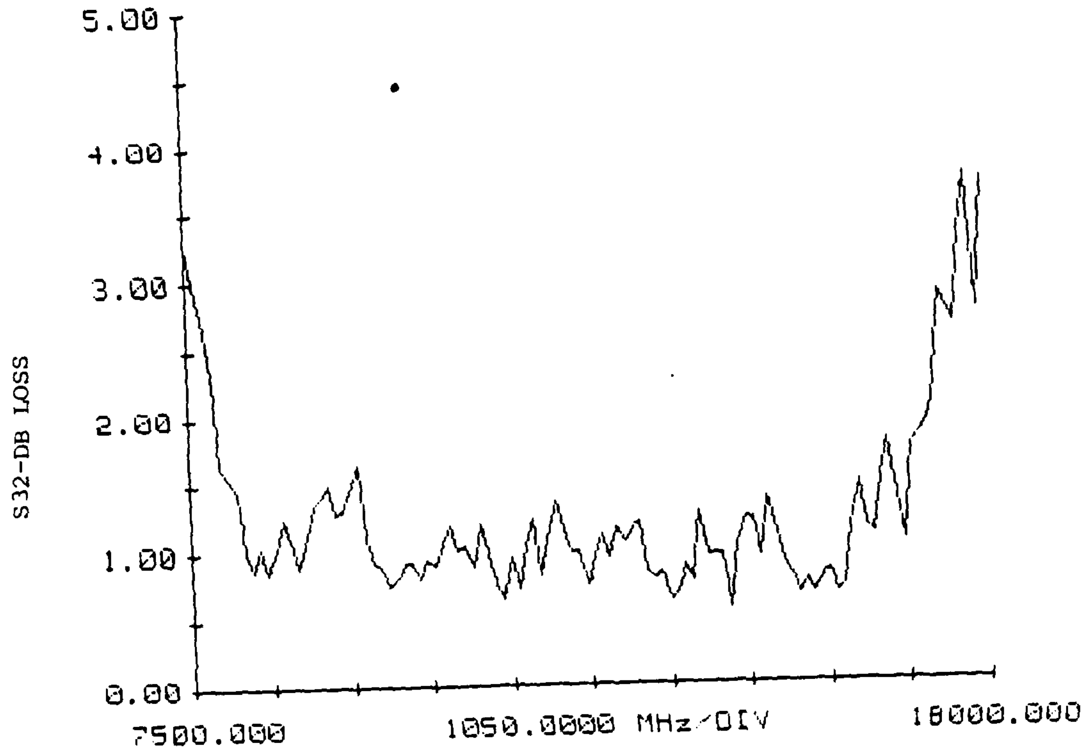

RAYTHEON CKuH40 PORT 2-4

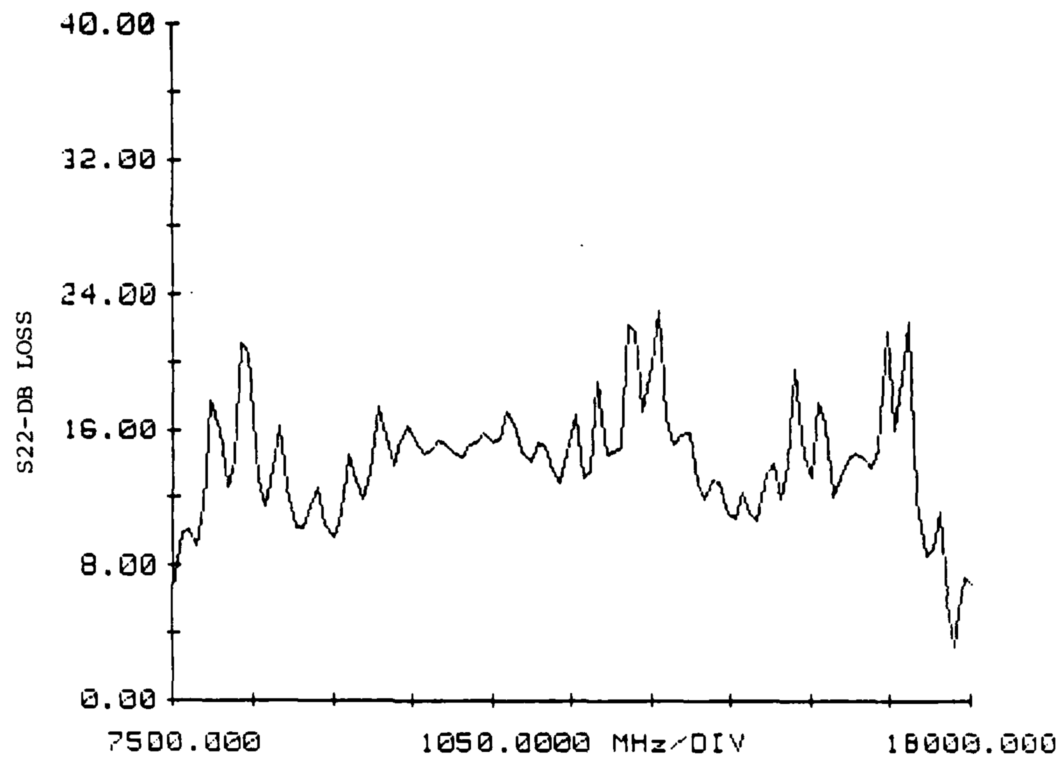

RAYTHEON CKuH40 PORT 2-4

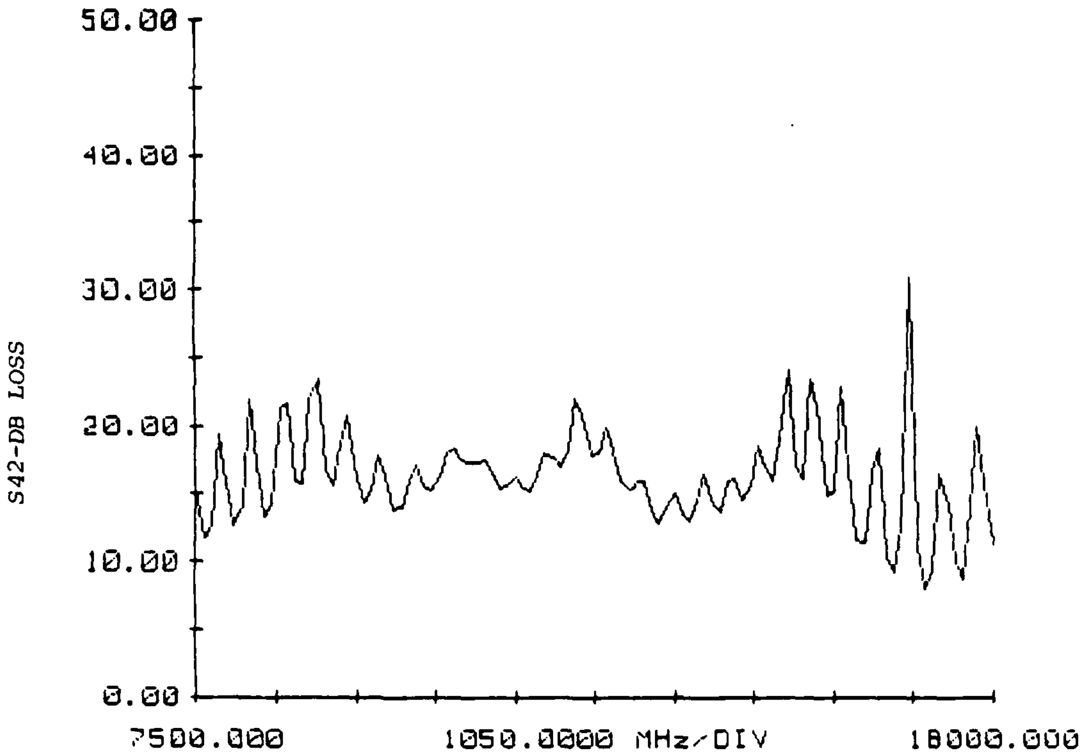

RAYTHEON CKuH40 PORT 3-1

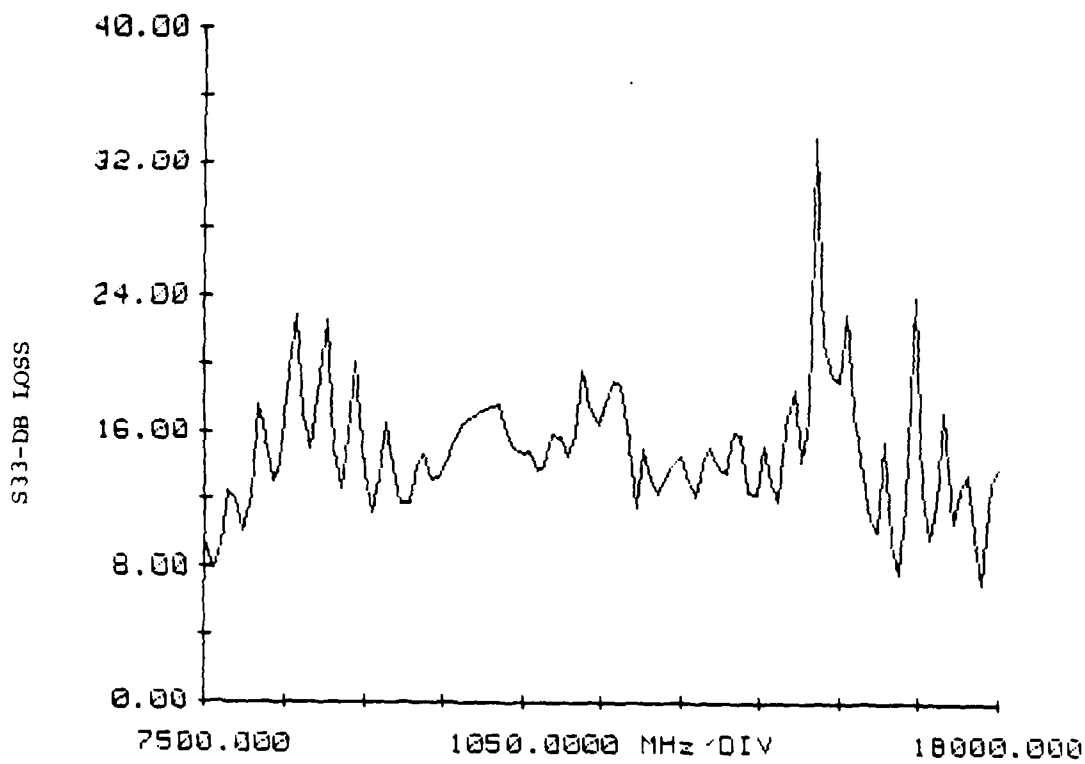

RAYTHEON CKuH40 PORT 3-1

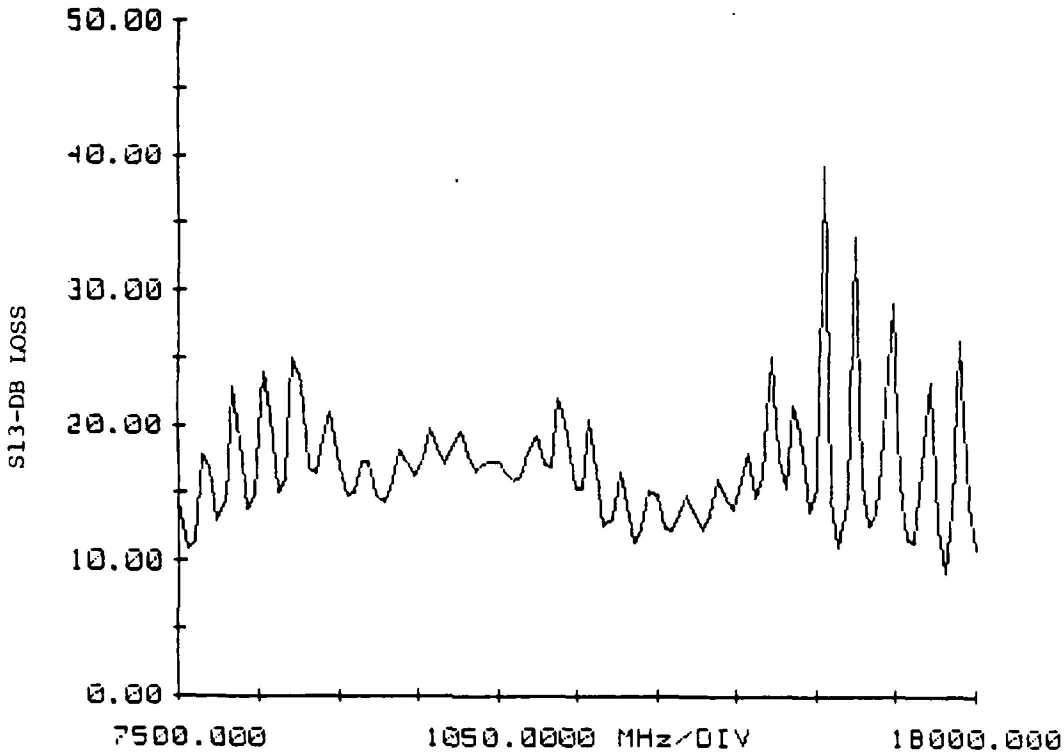

RAYTHEON CKuH40 PORT 3-2

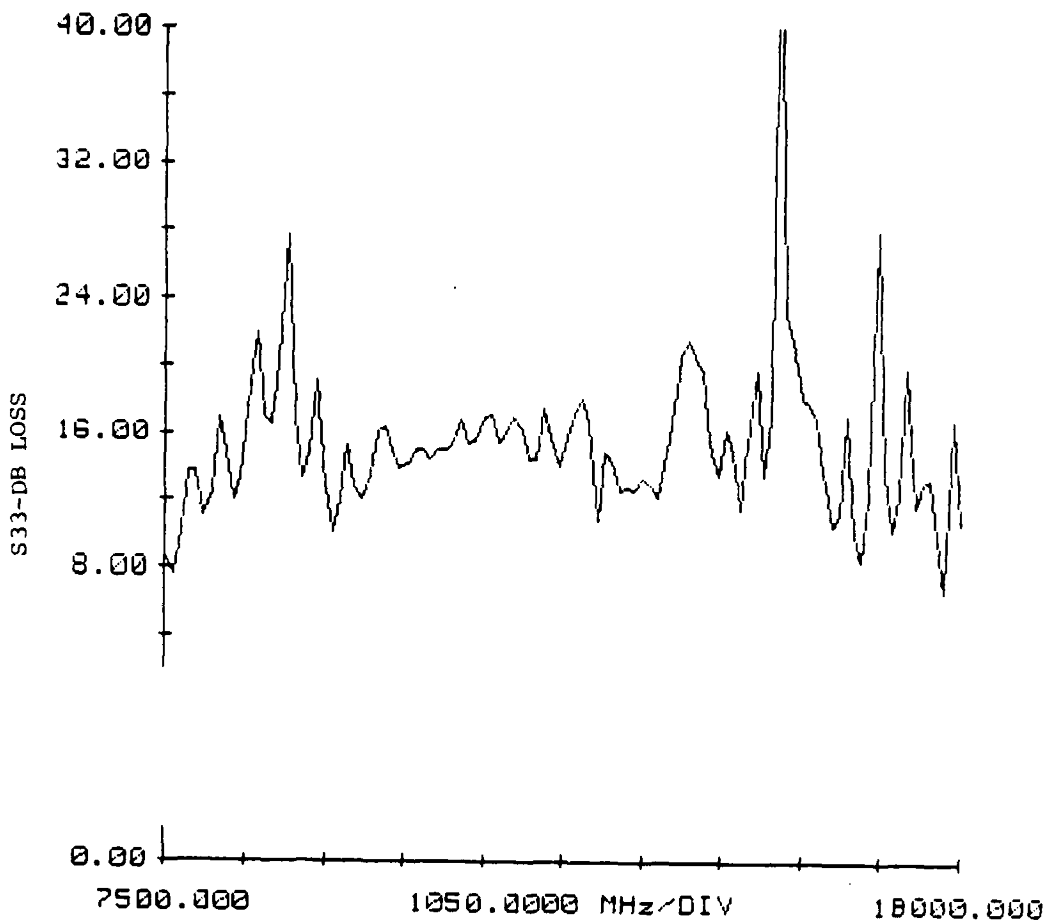

RAYTHEON CKuH40 PORT 3-2

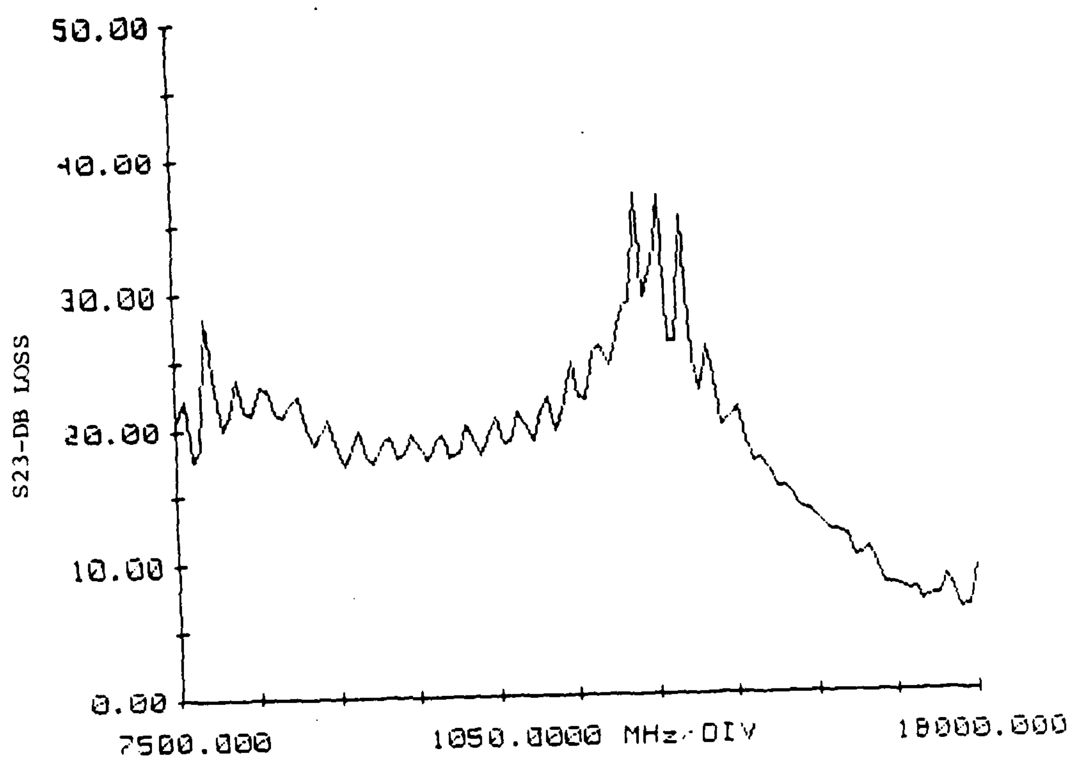

RAYTHEON CKuH40 PORT 3-4

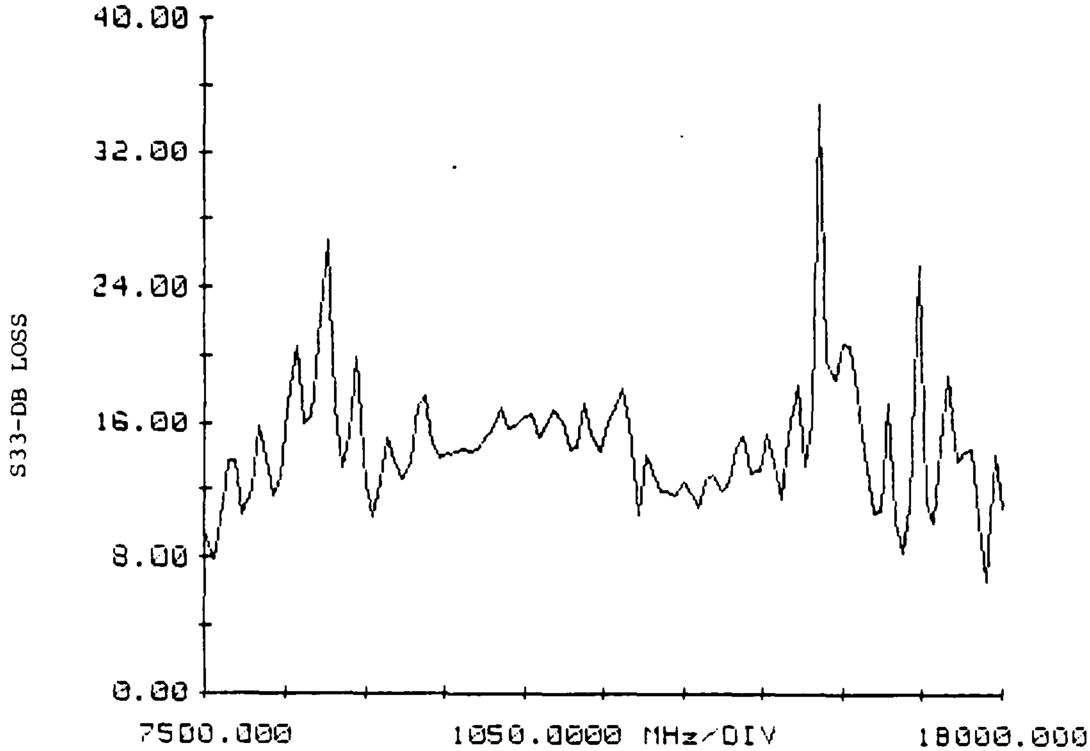

RAYTHEON CKuH40 PORT 3-4

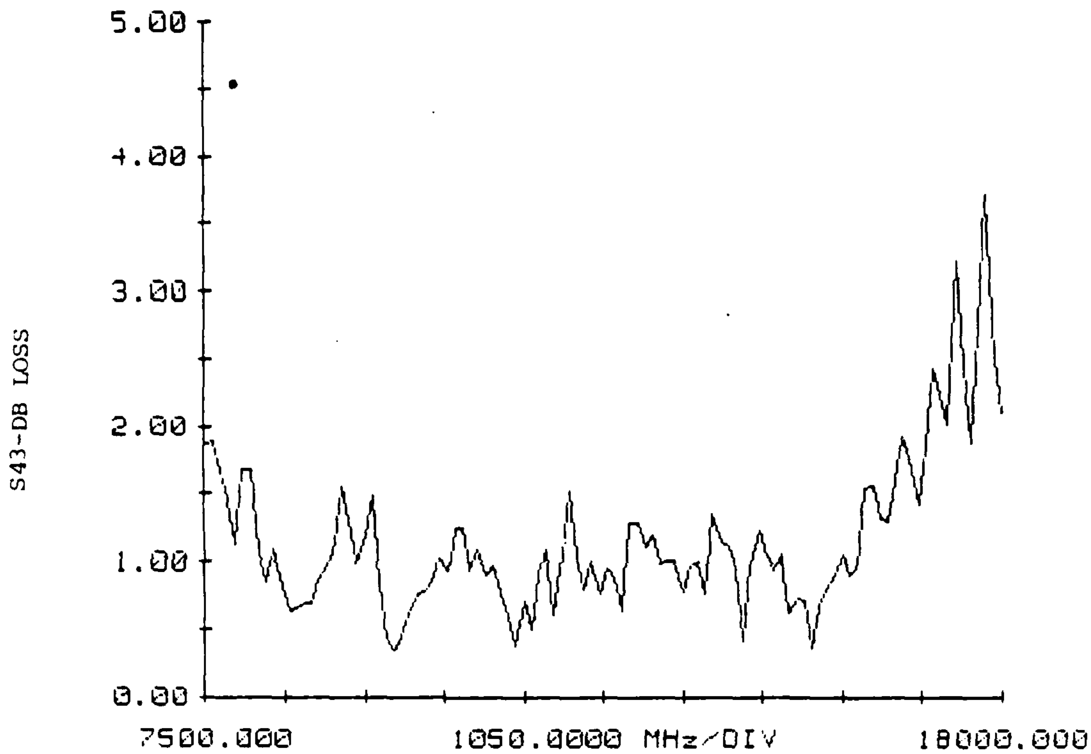

RAYTHEON CKuH40 PORT 4-1

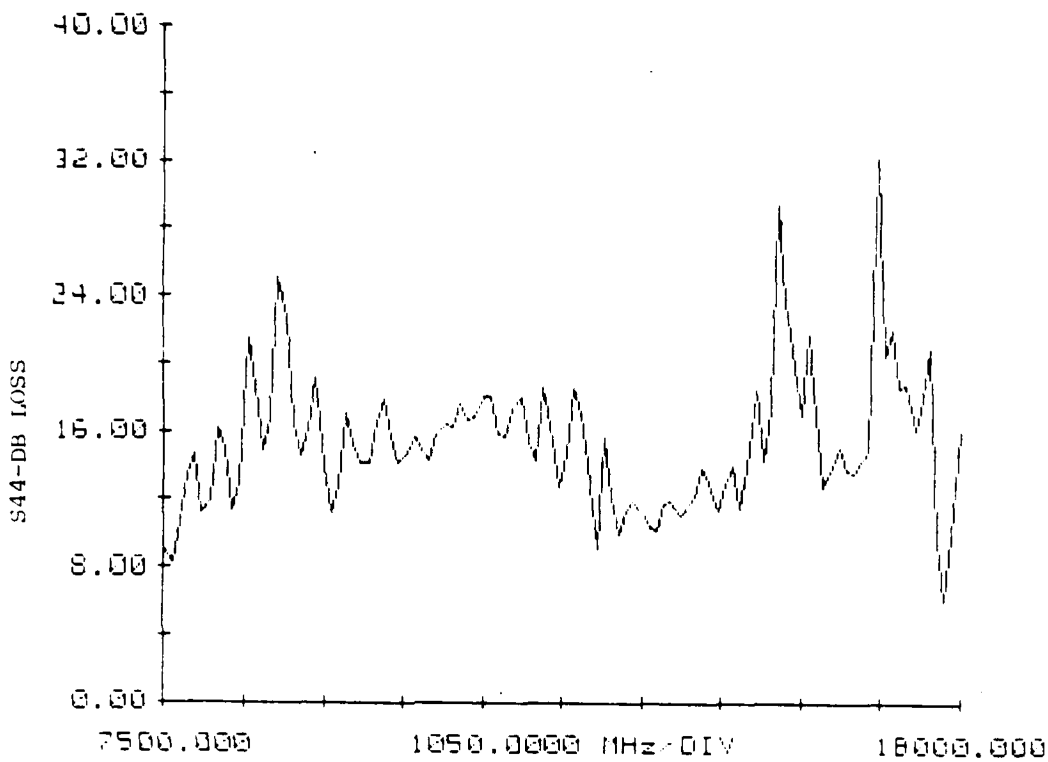

RAYTHEON CKuH40 PORT 4-1

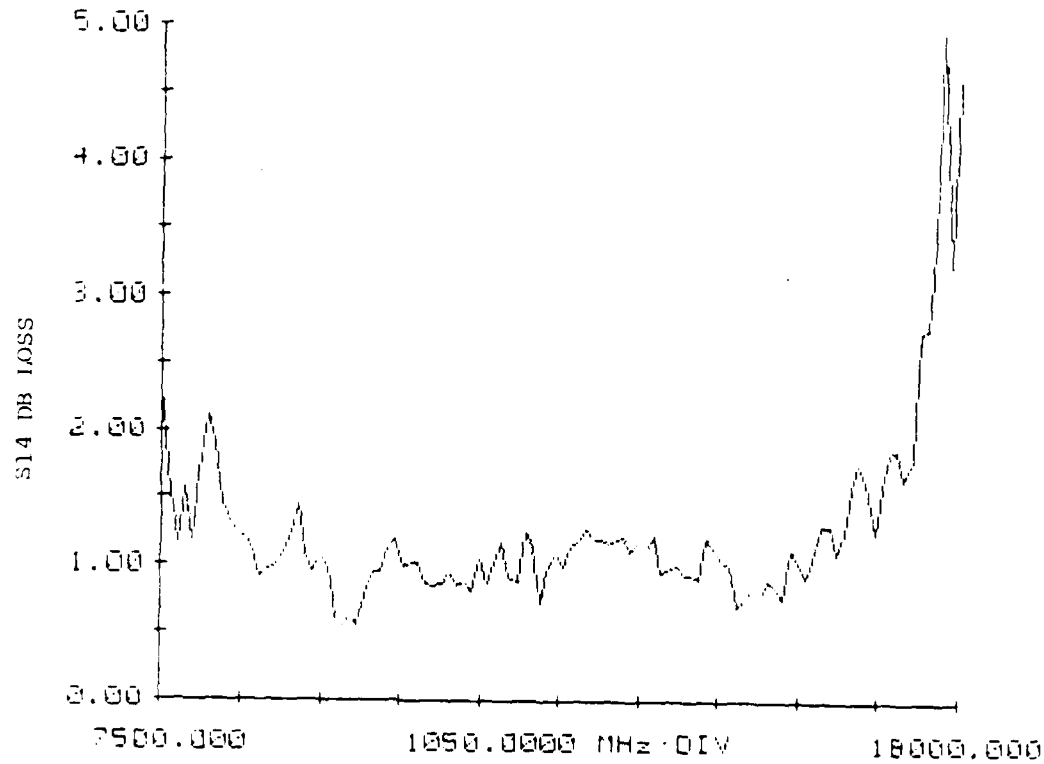

RAYTHEON CKuH40 PORT 4-2

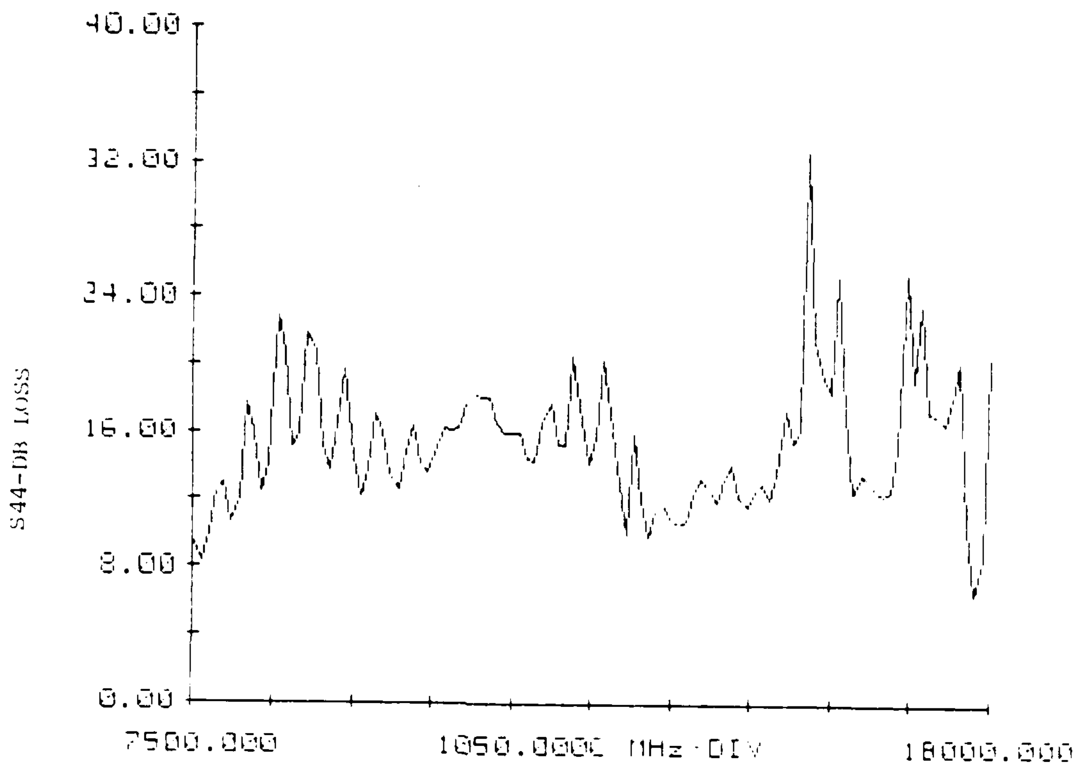

RAYTHEON CKuH40 PORT 4-2

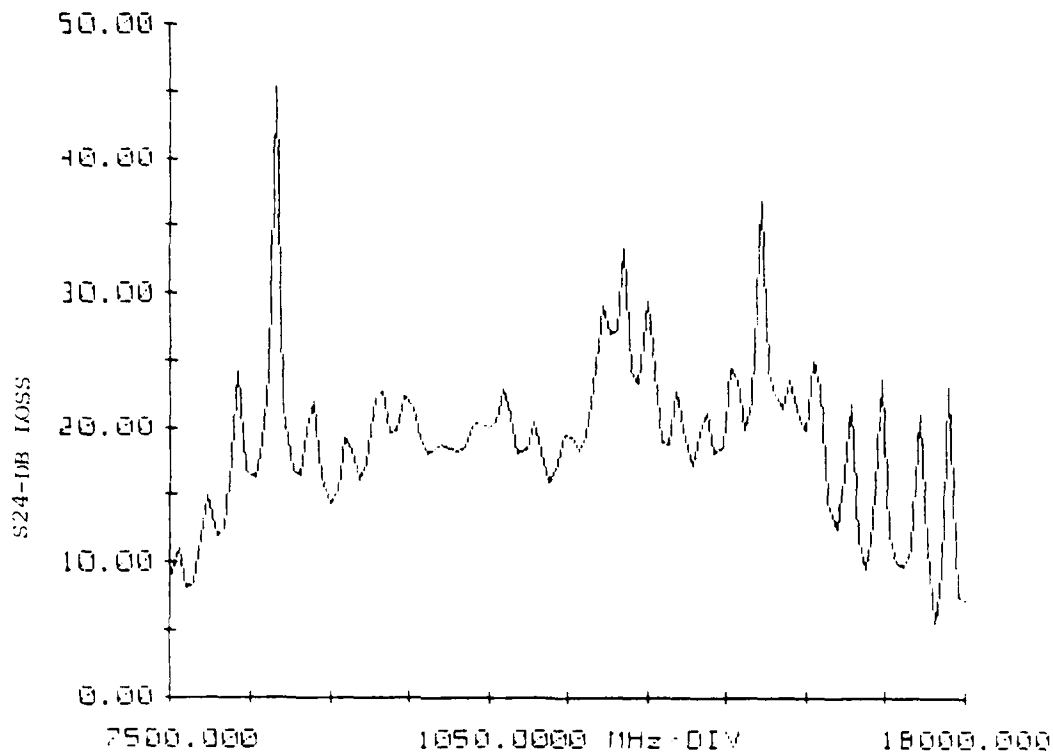

RAYTHEON CKuH40 PORT 4-3

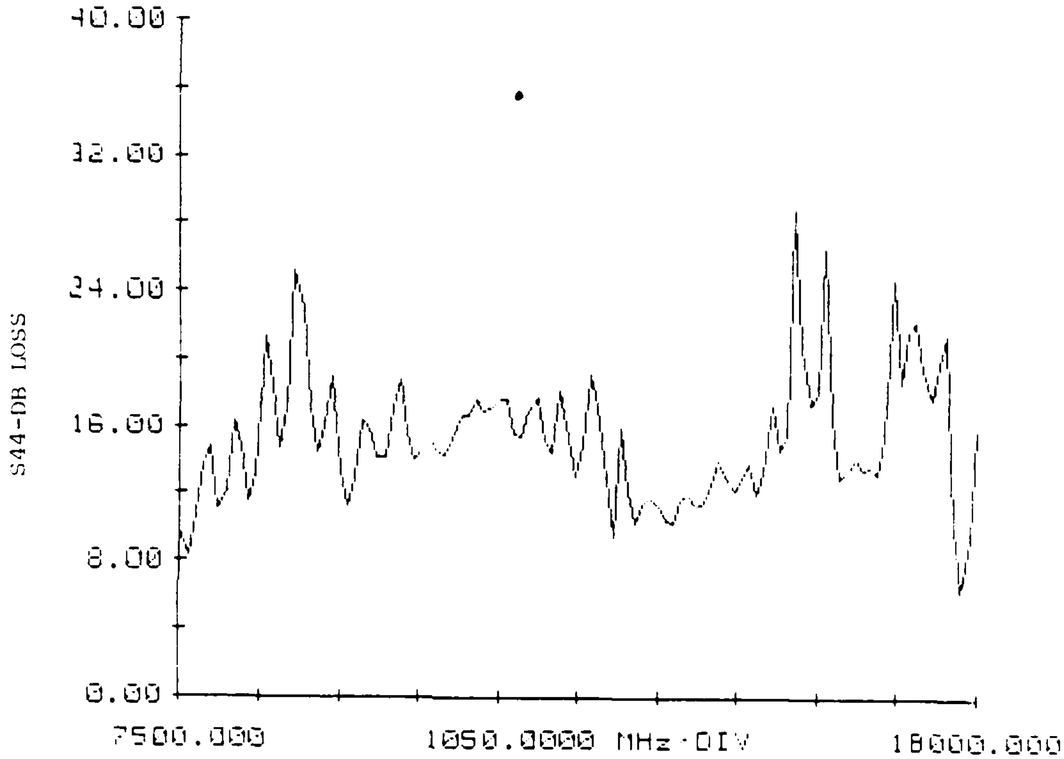

RAYTHEON CKuH40 PORT 4-3

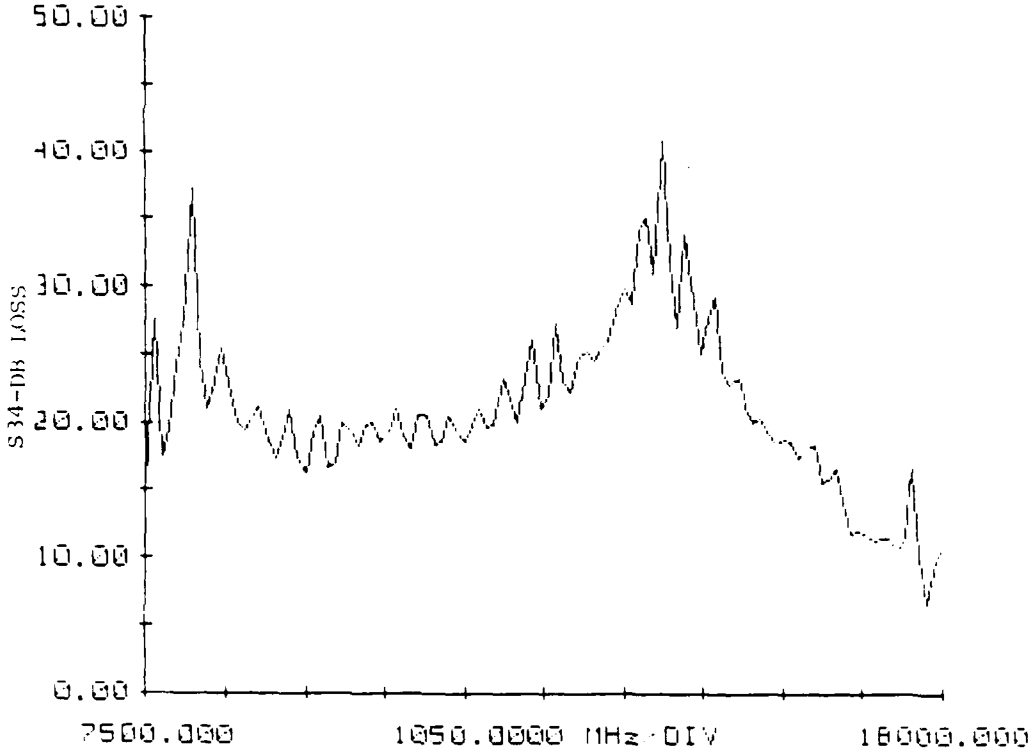

APPENDIX B

COMPUTER PROGRAM

```
10     REM Program "RIDGE" :
20     OPTION BASE 1
30     DIM Nbt(20),Pbt(20),Obt(20),Rbo(20)
40     COM A(7),E(7),F,K,Kk,Gama,Sat,Rem,B,D
50     Crit=.0001
60     Eps=.0001
70     Ea=1
80     M=0
90     N=0
100    A1=.259
110    A2=.014
120    A3=.035
130    A5=.050
140    A6=.020
150    A4=.173-(A2+A3+A5+A6)
160    A7=.259
170    B=.321
180    D=.1375
190    B1=.030
200    B2=D-2*B1
210    Ef=11.4
220    E1=1
230    E2=1
240    E3=13*.78
250    E4=1
260    E5=(2*B1+B2)/(2*B1/Ef+B2/Ea)
270    E6=1
280    E7=1
290    Upm=0
300    Gama=3.5
310    Sat=1820
320    Remp=1820
330    Remn=-Remp
340    Fi=8
350    Ff=16
360    Delf=1
370    A(1)=A1
380    A(2)=A2
390    A(3)=A3
400    A(4)=A4
410    A(5)=A5
420    A(6)=A6
430    A(7)=A7
440    E(1)=E1
450    E(2)=E2
460    E(3)=E3
470    E(4)=E4
480    E(5)=E5
490    E(6)=E6
500    E(7)=E7
510    IMAGE 4X,"A1",7X,"A2",7X,"A3",7X,"A4",7X,"A5",7X,"A6",7X,"A7"
520    PRINT USING 510
530    IMAGE 2X,7(DD.DDDD,2X)
540    PRINT USING 530;A1,A2,A3,A4,A5,A6,A7
550    IMAGE 4X,"E1",7X,"E2",7X,"E3",7X,"E4",7X,"E5",7X,"E6",7X,"E7"
560    PRINT USING 550
570    PRINT USING 530;E1,E2,E3,E4,E5,E6,E7
580    IMAGE 4X,"B",8X,"D",8X,"B1",7X,"Ef",6X,"Gama",6X,"Sat",6X,"Rem+"
590    PRINT USING 580
600    IMAGE 2X,5(DD.DDDD,2X),X,2(DDDD.D,3X),/
610    PRINT USING 600;B,D,B1,Ef,Gama,Sat,Remp
```

```
620   F=Fi
630   Rem=0
640 Lb1:  Rbt=6.8
650   Ibt=0
660   IF Sat=0 THEN GOTO Lb2
670   IMAGE /,"Rem=",MDDDD,5X,"***********",/
680   PRINT USING 670;Rem
690   Rem=Rem*.5*(1+B2/(B2+2*B1))
700 Lb2:  K=2*PI*F/11.8
710   Kk=K*K
720   CALL Newton(Rbt,Ibt,Crit,Eps)
730   M=M+1
740   IF Rem=0 THEN Lb3
750   GOTO Lb4
760 Lb3:  Rbo(M)=Rbt
770   Beta=Rbt
780   GOTO Lb5
790 Lb4:  Dbt=(Rbt-Rbo(M))*2*B1/D
800   Beta=Rbo(M)+Dbt
810 Lb5:  Phase=Beta*180/PI
820   IMAGE DD.DD," GHz",5X,"KY= ",D.DDDDE," /INCH",5X,"PHASE= ",D.DDDDE," DEG/I
NCH"
830   PRINT USING 820;F,Beta,Phase
840   IF Rem=0 THEN Lb7
850   IF Rem<0 THEN Lb6
860   Pbt(M)=Phase
870   GOTO Lb8
880 Lb6:  Nbt(M)=Phase
890   GOTO Lb8
900 Lb7:  Obt(M)=Phase
910 Lb8:  IF F=Ff THEN Lb9
920   F=F+Delf
930   GOTO Lb2
940 Lb9:  IF Rem<>0 THEN Lb10
950   Lg=720/(Obt(1)+Obt(M))/4
960   IMAGE "Quarter Wave Length=",D.DDDDE," INCH"
970   PRINT USING 960;Lg
980 Lb10:  IF Sat=0 THEN Lb99
990   N=N+1
1000  ON N GOTO Lb11,Lb12,Lb14
1010 Lb11: Rem=Remn
1020  GOTO Lb13
1030 Lb12: Rem=Remp
1040 Lb13: F=Fi
1050  M=0
1060  GOTO Lb1
1070 Lb14: M=1
1080  F=Fi
1090  PRINT LIN(1),"DIFFERENTIAL PHASE(DEG/INCH)"
1100  PRINT "FREQ(GHz)      B- - Bo      B+ - Bo      B- - B+"
1110 Lb15: Dnp=Nbt(M)-Pbt(M)
1120  Dno=Nbt(M)-Obt(M)
1130  Dpo=Pbt(M)-Obt(M)
1140  IMAGE X,DD.DD,7X,MDDD.DD,5X,MDDD.DD,5X,MDDD.DD
1150  PRINT USING 1140;F,Dno,Dpo,Dnp
1160  M=M+1
1170  F=F+Delf
1180  IF F<=Ff THEN Lb15
1190 Lb99: STOP
1200  END
1210  SUB Junct(Bc,K1,B,D)
1220  Ar=D/B
1230  Lc=2*PI/K1
1240  Cb=(4*Ar/(1-Ar^2))^2
1250  Apb=(1-(D/Lc)^2)^.5
1260  Apb=(1+Apb)/(1-Apb)
```

```
1270  Apb=Apb*((1+Ar)/(1-Ar))^(2/Ar)
1280  Apb=Apb+(3+Ar^2)/(1-Ar^2)
1290  Ab=(1-(B/Lc)^2)^.5
1300  Ab=(1+Ab)/(1-Ab)
1310  Ab=Ab*((1+Ar)/(1-Ar))^(2*Ar)
1320  Ab=Ab-(1+3*Ar^2)/(1-Ar^2)
1330  B1=(1-Ar^2)/(4*Ar)
1340  B1=B1*((1+Ar)/(1-Ar))^((Ar+1/Ar)/2)
1350  B1=LOG(B1)
1360  B2=2*(Ab+Apb+2*Cb)/(Ab*Apb-Cb^2)
1370  B3=( /(4*Lc))^2
1380  B3=F .*((1-Ar)/(1+Ar))^(4*Ar)
1390  B3=' 3*((5*Ar^2-1)/(1-Ar^2)+4*Cb*Ar^2/(3*Ab))^2
1400  Bc= *B/Lc*(B1+B2+B3)
1410  SUI .ND
1420  SU  Newton(Rbt,Ibt,Crit,Eps)
1430  I=1
1440  Id=1
1450 Ln1:  Rs=Rbt
1460  Is=Ibt
1470  IF Ibt>=0 THEN Ln2
1480  Is=-Ibt
1490 Ln2:  Ro=Rs
1500  Io=Is
1510 Ln3:  ON Id GOTO Ln4,Ln5
1520 Ln4: Rdel=Eps
1530  Idel=0
1540  GOTO Ln6
1550 Ln5:  Rdel=0
1560  Idel=Eps
1570  Id=1
1580 Ln6:  Rm=Ro-Rdel
1590  Im=Io-Idel
1600  Rp=Ro+Rdel
1610  Ip=Io+Idel
1620  Rbt=Ro
1630  Ibt=Io
1640  CALL Fund(Rbt,Ibt,Rr,Ir)
1650  CALL Cabs(Rr,Ir,Cr)
1660  IMAGE MD.DDDDE,4X,MD.DDDDE,6X,D.DDDDE
1680  IF Cr<Crit THEN Ret_main
1690  Rfo=Rr
1700  Ifo=Ir
1710  Rbt=Rm
1720  Ibt=Im
1730  CALL Fund(Rbt,Ibt,Rr,Ir)
1740  Rfm=Rr
1750  Ifm=Ir
1760  Rbt=Rp
1770  Ibt=Ip
1780  CALL Fund(Rbt,Ibt,Rr,Ir)
1790  Rfp=Rr
1800  Ifp=Ir
1810  Rfd=Rfo-Rfm
1820  Ifd=Ifo-Ifm
1830  CALL Cdiv(Rfd,Ifd,Rdel,Idel,Rfd,Ifd)
1840  Rfs=Rfm+Rfp-2*Rfo
1850  Ifs=Ifm+Ifp-2*Ifo
1860  CALL Cmult(Rdel,Idel,Rdel,Idel,Rdels,Idels)
1870  CALL Cdiv(Rfs,Ifs,Rdels,Idels,Rfs,Ifs)
1880  CALL Cabs(Rfs,Ifs,Cfs)
1890  IF Cfs<.0000001 THEN Ln9
1900  ON Id GOTO Ln7,Ln8
1910 Ln7:  Id=2
1920  IF I>10 THEN Ln11
1930  I=I+1
```

```
1940  GOTO Ln3
1950 Ln8:  GOTO Ln10
1960 Ln9:  CALL Cmult(Rfo,Ifo,Rfs,Ifs,Ros,Ios)
1970  CALL Cmult(Rfd,Ifd,Rfd,Ifd,Rdd,Idd)
1980  CALL Cdiv(Ros,Ios,Rdd,Idd,Rosd,Iosd)
1990  Rosd=1-2*Rosd
2000  Iosd=-2*Iosd
2010  CALL Csqrt(Rosd,Iosd,Rcosd,Icosd)
2020  Rcosd=1-Rcosd
2030  Icosd=-Icosd
2040  CALL Cmult(Rfd,Ifd,Rcosd,Icosd,Rdz,Idz)
2050  CALL Cdiv(Rdz,Idz,Rfs,Ifs,Rdzz,Idzz)
2060  Rdz=-Rdzz
2070  Idz=-Idzz
2080  CALL Cabs(Rdz,Idz,Cdz)
2090  IF Cdz<.0000001 THEN Ln11
2100  Rbt=Rs+Rdz
2110  Ibt=Is+Idz
2120  IF I>10 THEN Ln11
2130  I=I+1
2140  GOTO Ln1
2150 Ln10: PRINT "ZERO DERIVATIVE"
2160  GOTO Ret_main
2170 Ln11:  IMAGE "DIVERGENCE OF ITERATION PROCESS: f(x)=",D.DDDDE
2180  PRINT USING 2170;Cr
2190 Ret_main: SUBEXIT
2200  SUBEND
2210  SUB Cmult(X1,Y1,X2,Y2,X3,Y3)
2220  X3=X1*X2-Y1*Y2
2230  Y3=X1*Y2+Y1*X2
2240  SUBEND
2250  SUB Cdiv(X1,Y1,X2,Y2,X3,Y3)
2260  Denom=X2*X2+Y2*Y2
2270  X3=(X1*X2+Y1*Y2)/Denom
2280  Y3=(Y1*X2-X1*Y2)/Denom
2290  SUBEND
2300  SUB Cabs(X,Y,Rm)
2310  Rm=(X*X+Y*Y)^.5
2320  SUBEND
2330  SUB Csin(X1,Y1,X2,Y2)
2340  X2=SIN(X1)*(EXP(Y1)+EXP(-Y1))/2
2350  Y2=COS(X1)*(EXP(Y1)-EXP(-Y1))/2
2360  SUBEND
2370  SUB Ccos(X1,Y1,X2,Y2)
2380  X2=COS(X1)*(EXP(Y1)+EXP(-Y1))/2
2390  Y2=-SIN(X1)*(EXP(Y1)-EXP(-Y1))/2
2400  SUBEND
2410  SUB Csqrt(X1,Y1,X2,Y2)
2420  Mag=(X1*X1+Y1*Y1)^.25
2430  IF X1<0 THEN Lba1
2440  IF X1=0 THEN Lba2
2450  Ang=ATN(Y1/X1)/2
2460  GOTO Lcsq
2470 Lba1: Ang=(PI+ATN(Y1/X1))/2
2480  GOTO Lcsq
2490 Lba2:  IF Y1<0 THEN Lba3
2500  Ang=PI/4
2510  GOTO Lcsq
2520 Lba3: Ang=-PI/4
2530 Lcsq: X2=Mag*COS(Ang)
2540  Y2=Mag*SIN(Ang)
2550  SUBEND
2560  SUB Fund(Rbt,Ibt,Rr,Ir)
2570  DIM Rkx(7),Ikx(7),Rsn(7),Isn(7),Rcn(7),Icn(7)
2580  DIM Rma(11),Ima(11),Rmb(11),Imb(11),Rmc(11),Imc(11),Rmd(11),Imd(11)
2590  COM A(*),E(*),F,K,Kk,Gama,Sat,Rem,B,D
```

```
2600  R0=0
2610  I1=1
2620  CALL Cmult(Rbt,Ibt,Rbt,Ibt,Rbts,Ibts)
2630  FOR I=1 TO 7
2640  Rkx=Kk*E(I)-Rbts
2650  Ikx=-Ibts
2660  CALL Csqrt(Rkx,Ikx,Rkx(I),Ikx(I))
2670  IF Ikx(I)>0 THEN CALL Neg(Rkx(I),Ikx(I),Rkx(I),Ikx(I))
2680  NEXT I
2690  U=1
2700  Rxxy=0
2710  Ixxy=0
2720  IF Sat=0 THEN Lbb1
2730  U=1/3+2*(1-(Gama*Sat/(F*1000))^2)^.5/3
2740  U=U+(1-U)*ABS(Rem/Sat)^1.5
2750  U=1
2760  Ixxy=Gama*Rem/(F*1000)
2770 Lbb1: Rho=U/(U*U-Ixxy^2)
2780  Iteta=Ixxy/U
2790  Rkx=Kk*E(5)/Rho-Rbts
2800  CALL Csqrt(Rkx,Ikx,Rkx(5),Ikx(5))
2810  IF Ikx(5)>0 THEN CALL Neg(Rkx(5),Ikx(5),Rkx(5),Ikx(5))
2820  Kx1=Rkx(1)
2830  Bc=0
2840  IF Kx1<=0 THEN Lbb2
2850  IF D=B THEN Lbb2
2860  CALL Junct(Bc,Kx1,B,D)
2870  Bc=-Bc*Kx1/K
2880 Lbb2: FOR I=1 TO 7
2890  Rkxa=Rkx(I)*A(I)
2900  Ikxa=Ikx(I)*A(I)
2910  CALL Csin(Rkxa,Ikxa,Rsn,Isn)
2920  Rsn(I)=Rsn
2930  Isn(I)=Isn
2940  CALL Ccos(Rkxa,Ikxa,Rcn,Icn)
2950  Rcn(I)=Rcn
2960  Icn(I)=Icn
2970  Rma(I)=Rcn
2980  Ima(I)=Icn
2990  CALL Cmult(Rkx(I),Ikx(I),Rsn,Isn,Rkxsn,Ikxsn)
3000  CALL Cmult(R0,I1,Rkxsn,Ikxsn,Rmb,Imb)
3010  Rmb(I)=-Rmb/K
3020  Imb(I)=-Imb/K
3030  CALL Cdiv(Rsn,Isn,Rkx(I),Ikx(I),Rsnkx,Isnkx)
3040  CALL Cmult(R0,I1,Rsnkx,Isnkx,Rmc,Imc)
3050  Rmc(I)=-K*Rmc
3060  Imc(I)=-K*Imc
3070  Rmd(I)=Rma(I)
3080  Imd(I)=Ima(I)
3090  NEXT I
3100  Rma(11)=Rma(7)
3110  Ima(11)=Ima(7)
3120  Rmb(11)=Rmb(7)
3130  Imb(11)=Imb(7)
3140  Rmc(11)=Rmc(7)
3150  Imc(11)=Imc(7)
3160  Rmd(11)=Rmd(7)
3170  Imd(11)=Imd(7)
3180  Rma(10)=1
3190  Ima(10)=0
3200  Rmb(10)=0
3210  Imb(10)=Bc
3220  Rmc(10)=0
3230  Imc(10)=0
3240  Rmd(10)=1
3250  Imd(10)=0
```

```
3260  Rma(9)=D
3270  Ima(9)=0
3280  Rmb(9)=0
3290  Imb(9)=0
3300  Rmc(9)=0
3310  Imc(9)=0
3320  Rmd(9)=B
3330  Imd(9)=0
3340  Rma(8)=Rma(6)
3350  Ima(8)=Ima(6)
3360  Rmb(8)=Rmb(6)
3370  Imb(8)=Imb(6)
3380  Rmc(8)=Rmc(6)
3390  Imc(8)=Imc(6)
3400  Rmd(8)=Rmd(6)
3410  Imd(8)=Imd(6)
3420  CALL Cdiv(Rsn(5),Isn(5),Rkx(5),Ikx(5),Rsnkx5,Isnkx5)
3430  CALL Cmult(R0,I1,Rsnkx5,Isnkx5,Rsk5,Isk5)
3440  CALL Cmult(Rbt,Ibt,Rsk5,Isk5,Rsk,Isk)
3450  CALL Cmult(R0,Iteta,Rsk,Isk,Rskk,Iskk)
3460  CALL Cmult(Rkx(5),Ikx(5),Rkx(5),Ikx(5),Rkx5s,Ikx5s)
3470  Rxtk=-Rbts*Iteta^2-Rkx5s
3480  Ixtk=-Ibts*Iteta^2-Ikx5s
3490  CALL Cmult(Rxtk,Ixtk,Rsk5,Isk5,Rtk,Itk)
3500  Rma(7)=Rcn(5)-Rskk
3510  Ima(7)=Icn(5)-Iskk
3520  Rmb(7)=Rho*Rtk/K
3530  Imb(7)=Rho*Itk/K
3540  Rmc(7)=-K*Rsk5/Rho
3550  Imc(7)=-K*Isk5/Rho
3560  Rmd(7)=Rcn(5)+Rskk
3570  Imd(7)=Icn(5)+Iskk
3580  Rma(6)=Rma(4)
3590  Ima(6)=Ima(4)
3600  Rmb(6)=Rmb(4)
3610  Imb(6)=Imb(4)
3620  Rmc(6)=Rmc(4)
3630  Imc(6)=Imc(4)
3640  Rmd(6)=Rmd(4)
3650  Imd(6)=Imd(4)
3660  Rma(5)=Rma(3)
3670  Ima(5)=Ima(3)
3680  Rmb(5)=Rmb(3)
3690  Imb(5)=Imb(3)
3700  Rmc(5)=Rmc(3)
3710  Imc(5)=Imc(3)
3720  Rmd(5)=Rmd(3)
3730  Imd(5)=Imd(3)
3740  Rma(4)=Rma(2)
3750  Ima(4)=Ima(2)
3760  Rmb(4)=Rmb(2)
3770  Imb(4)=Imb(2)
3780  Rmc(4)=Rmc(2)
3790  Imc(4)=Imc(2)
3800  Rmd(4)=Rmd(2)
3810  Imd(4)=Imd(2)
3820  Rma(3)=B
3830  Ima(3)=0
3840  Rmb(3)=0
3850  Imb(3)=0
3860  Rmc(3)=0
3870  Imc(3)=0
3880  Rmd(3)=D
3890  Imd(3)=0
3900  Rma(2)=1
3910  Ima(2)=0
```

```
3920  Rmb(2)=0
3930  Imb(2)=Bc
3940  Rmc(2)=0
3950  Imc(2)=0
3960  Rmd(2)=1
3970  Imd(2)=0
3980  Rxa=Rma(1)
3990  Ixa=Ima(1)
4000  Rxb=Rmb(1)
4010  Ixb=Imb(1)
4020  Rxc=Rmc(1)
4030  Ixc=Imc(1)
4040  Rxd=Rmd(1)
4050  Ixd=Imd(1)
4060  FOR I=2 TO 11
4070  CALL Cmult(Rxa,Ixa,Rma(I),Ima(I),Raa,Iaa)
4080  CALL Cmult(Rxb,Ixb,Rmc(I),Imc(I),Rbc,Ibc)
4090  Rta=Raa+Rbc
4100  Ita=Iaa+Ibc
4110  CALL Cmult(Rxa,Ixa,Rmb(I),Imb(I),Rab,Iab)
4120  CALL Cmult(Rxb,Ixb,Rmd(I),Imd(I),Rbd,Ibd)
4130  Rtb=Rab+Rbd
4140  Itb=Iab+Ibd
4150  CALL Cmult(Rxc,Ixc,Rma(I),Ima(I),Rca,Ica)
4160  CALL Cmult(Rxd,Ixd,Rmc(I),Imc(I),Rdc,Idc)
4170  Rtc=Rca+Rdc
4180  Itc=Ica+Idc
4190  CALL Cmult(Rxc,Ixc,Rmb(I),Imb(I),Rcb,Icb)
4200  CALL Cmult(Rxd,Ixd,Rmd(I),Imd(I),Rdd,Idd)
4210  Rtd=Rcb+Rdd
4220  Itd=Icb+Idd
4230  Rxa=Rta
4240  Ixa=Ita
4250  Rxb=Rtb
4260  Ixb=Itb
4270  Rxc=Rtc
4280  Ixc=Itc
4290  Rxd=Rtd
4300  Ixd=Itd
4310  NEXT I
4320  Rr=Rxc
4330  Ir=Ixc
4340  SUBEND
4350  SUB Neg(X1,Y1,X2,Y2)
4360  X2=-X1
4370  Y2=-Y1
4380  SUBEND
```

END

DATE
FILMED

9 — 83

DTIC